BRITISH STANDARD

BS ISO 24173:2009

Microbeam analysis — Guidelines for orientation measurement using electron backscatter diffraction

ICS 71.040.50

BSi

British Standards

National foreword

This British Standard is the UK implementation of ISO 24173:2009.

The UK participation in its preparation was entrusted to Technical Committee CII/9, Microbeam analysis.

A list of organizations represented on this committee can be obtained on request to its secretary.

This publication does not purport to include all the necessary provisions of a contract. Users are responsible for its correct application.

Compliance with a British Standard cannot confer immunity from legal obligations.

Amendments/corrigenda issued since publication

Date	Comments

BS ISO 24173:2009

INTERNATIONAL STANDARD

ISO
24173

First edition
2009-09-01

Microbeam analysis — Guidelines for orientation measurement using electron backscatter diffraction

Analyse par microfaisceaux — Lignes directrices pour la mesure d'orientation par diffraction d'électrons rétrodiffusés

Contents

Page

iii

Foreword

ISO (the International Organization for Standardization) is a worldwide federation of national standards bodies (ISO member bodies). The work of preparing International Standards is normally carried out through ISO technical committees. Each member body interested in a subject for which a technical committee has been established has the right to be represented on that committee. International organizations, governmental and non-governmental, in liaison with ISO, also take part in the work. ISO collaborates closely with the International Electrotechnical Commission (IEC) on all matters of electrotechnical standardization.

International Standards are drafted in accordance with the rules given in the ISO/IEC Directives, Part 2.

The main task of technical committees is to prepare International Standards. Draft International Standards adopted by the technical committees are circulated to the member bodies for voting. Publication as an International Standard requires approval by at least 75 % of the member bodies casting a vote.

Attention is drawn to the possibility that some of the elements of this document may be the subject of patent rights. ISO shall not be held responsible for identifying any or all such patent rights.

ISO 24173 was prepared by Technical Committee ISO/TC 202, *Microbeam analysis*.

Introduction

Electron backscatter diffraction (EBSD) is a technique that is used with a scanning electron microscope (SEM), a combined SEM-FIB (focussed-ion beam) microscope or an electron probe microanalyser (EPMA) to measure and map local crystallography in crystalline specimens [1],[2].

Electron backscatter patterns (EBSPs) are formed when a stationary electron beam strikes the surface of a steeply inclined specimen, which is usually tilted at ≈ 70° from normal to the electron beam. EBSPs are imaged via an EBSD detector, which comprises a scintillator (such as a phosphor screen or a YAG single crystal) and a low-light-level camera (normally a charge-coupled device, CCD). Patterns are occasionally imaged directly on photographic film.

By analysing the EBSPs, it is possible to measure the orientation of the crystal lattice and, in some cases, to identify also the phase of the small volume of crystal under the electron beam. EBSD is a surface diffraction effect where the signal arises from a depth of just a few tens of nanometres, so careful specimen preparation is essential for successful application of the technique [3].

In a conventional SEM with a tungsten filament, a spatial resolution of about 0,25 µm can be achieved; however, with a field-emission gun SEM (FEG-SEM), the resolution limit is 10 nm to 50 nm, although the value is strongly dependent on both the material being examined and on the instrument operating parameters. Orientation measurements in test specimens can be carried out with an accuracy of ≈ 0,5°.

By scanning the electron beam over a region of the specimen surface whilst simultaneously acquiring and analysing EBSPs, it is possible to produce maps that show the spatial variation of orientation, phase, EBSP quality and other related measures. These data can be used for quantitative microstructural analysis to measure, for example, the average grain size (and in some cases the size distribution), the crystallographic texture (distribution of orientations) or the amount of boundaries with special characteristics (e.g. twin boundaries). EBSD can provide three-dimensional microstructural characterization by its use in combination with an accurate serial sectioning technique, such as focussed-ion beam milling [4].

It is strongly recommended that EBSD users be well acquainted with both the principles of crystallography and the various methods for representing orientations (both of which are described in the existing literature in this field) in order to make best use of the EBSD technique and the data produced [5],[6].

INTERNATIONAL STANDARD

Microbeam analysis — Guidelines for orientation measurement using electron backscatter diffraction

IMPORTANT — The electronic file of this document contains colours which are considered to be useful for the correct understanding of the document. Users should therefore consider printing this document using a colour printer.

1   Scope

This International Standard gives advice on how to generate reliable and reproducible crystallographic orientation measurements using electron backscatter diffraction (EBSD). It addresses the requirements for specimen preparation, instrument configuration, instrument calibration and data acquisition.

2   Normative references

The following referenced documents are indispensable for the application of this document. For dated references, only the edition cited applies. For undated references, the latest edition of the referenced document (including any amendments) applies.

ISO/IEC 17025, *General requirements for the competence of testing and calibration laboratories*

ISO/IEC Guide 98-3, *Uncertainty of measurement — Part 3: Guide to the expression of uncertainty in measurement (GUM:1995)*

3   Terms and definitions

For the purposes of this document, the following terms and definitions apply.

3.1
crystal
entity consisting of a regular, repeated arrangement of atoms in space and usually described by a space group, a crystal system, unit cell parameters (including the lengths and angles between the unit cell axes) and the positions of the atoms inside the unit cell [7],[8]

NOTE 1   For example, an aluminium crystal can be represented by a cube (unit cell) of length 0,404 94 nm along each edge and with atoms at the corners and centres of the cube faces.

NOTE 2   Simulations of the atomic arrangement in a small ($4 \times 4 \times 4$ unit cells) aluminium crystal, as viewed along the [1 0 0], [1 1 1] and [1 1 0] directions, are shown in Figure 1, together with the associated spherical Kikuchi patterns for each crystal orientation. The 4-fold, 3-fold and 2-fold crystal symmetries are easily seen, as are the mirror planes.

NOTE 3   For those unfamiliar with crystallography, it is recommended that a standard textbook be consulted (see for example References [7], [8] and [9]).

NOTE 4   Annex C contains a brief introduction to crystallography and a guide to the indexing of EBSPs for materials with cubic crystal symmetry.

[100]   [111]   [110]
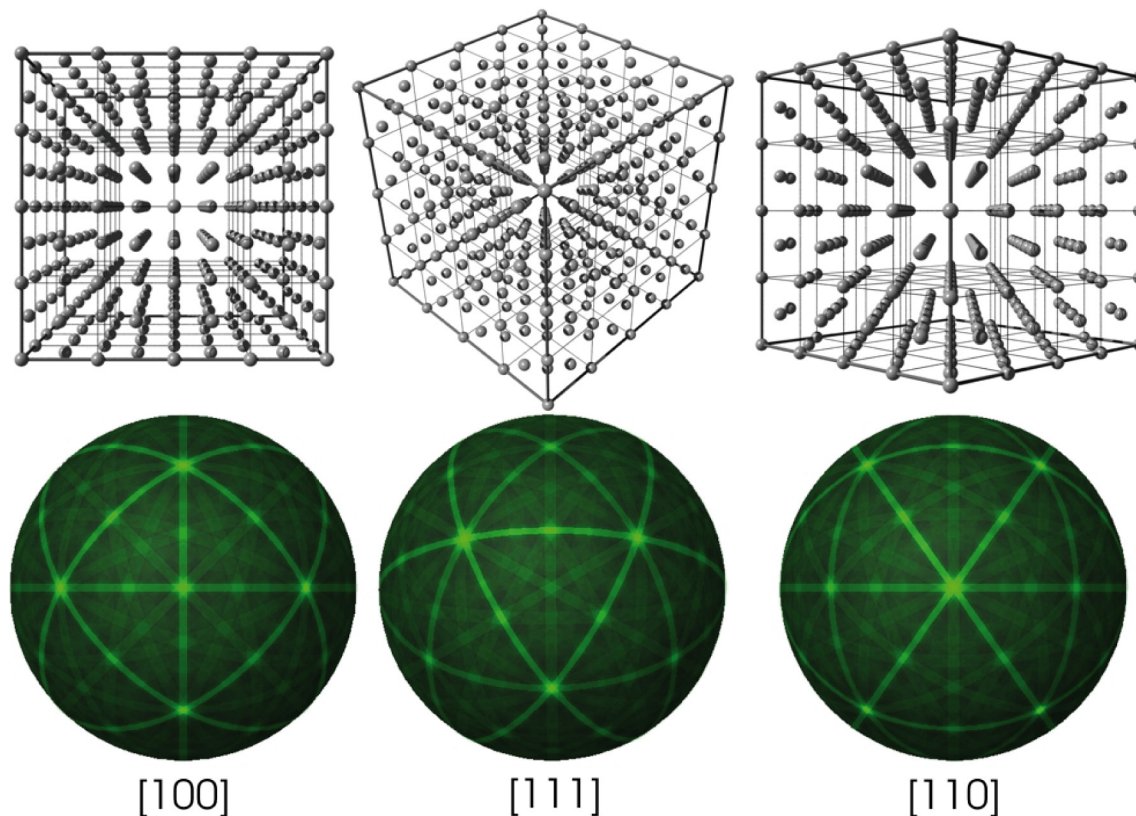
Figure 1 — Simulations of a small aluminium crystal (top) as viewed along the [1 0 0], [1 1 1] and [1 1 0] directions, with their associated spherical Kikuchi patterns (bottom). The symmetry is clearly shown.

3.2
crystal plane
plane, usually denoted as ($h\,k\,l$), representing the intersection of a plane with the a-, b- and c-axes of the unit cell at distances of $1/h$, $1/k$ and $1/l$, where h, k, and l are integers

NOTE 1   The integers h, k, and l are usually referred to as the Miller indices of a crystal plane.

NOTE 2   See Annex C for more information.

3.3
crystal direction
direction, usually denoted as [$u\,v\,w$], representing a vector direction in multiples of the basis vectors describing the a, b and c crystal axes

NOTE   See Annex C for more information.

3.4
crystal unit cell
cell which is repeated (infinitely) to build up the crystal

NOTE   It is usually defined by three lengths, a, b and c, and three angles, α, β and γ. The lengths are usually given in ångströms or nanometres and the angles in degrees.

3.5
crystallographic orientation
alignment of the crystal coordinate system (for example, [1 0 0], [0 1 0], [0 0 1] for a cubic crystal) in relation to the specimen coordinate system

NOTE   The specimen coordinate system can be denoted as X, Y, Z. When EBSD is applied to the study of rolled materials, it is often denoted as RD, TD, ND [RD = reference (or rolling) direction, TD = transverse direction and ND = normal direction].

3.6
EBSD detector
detector used to capture the electron backscatter pattern and convert it to an image visible on the display device (computer screen) via a video-camera, which is commonly a high-sensitivity charged-coupled device (CCD)

NOTE   See also 3.21.

3.7
electron backscatter diffraction
EBSD
diffraction process that arises between the backscattered electrons and the atomic planes of a highly tilted crystalline specimen when illuminated by a stationary incident electron beam

NOTE   Commonly used alternative terms for EBSD are "EBSP" (or more usually the "EBSP technique") (see 3.8), "BKD" (backscattered Kikuchi diffraction), "BKED" (backscattered Kikuchi electron diffraction) and "BKDP" (backscattered Kikuchi diffraction pattern).

3.8
electron backscatter pattern
EBSP
intersecting array of quasi-linear features, known as Kikuchi bands (see Figure 2), produced by electron backscatter diffraction and recorded using a suitable detector, for example observed on a phosphorescent screen or, less commonly, on photographic film
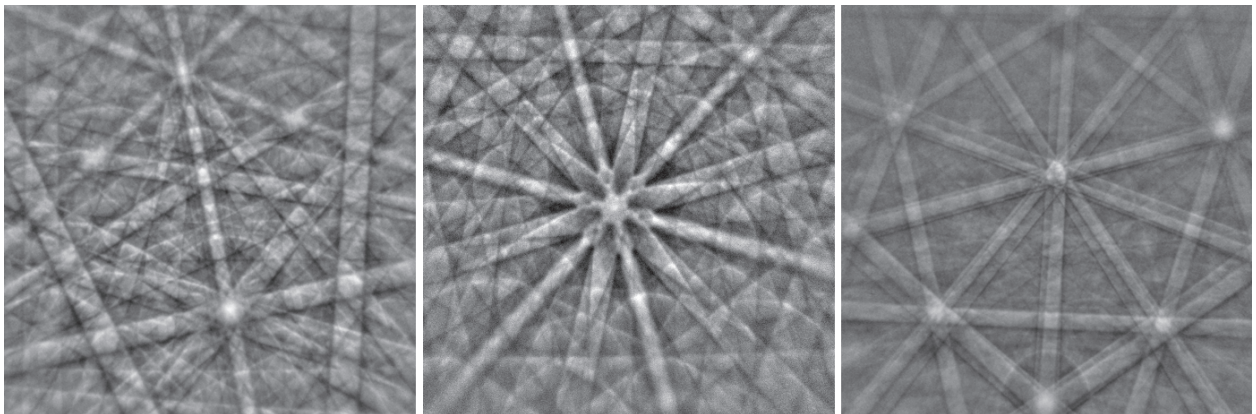
Figure 2 — Examples of EBSPs showing arrays of overlapping Kikuchi bands

3.9
EBSD grain
region, with similar orientation, delineated by boundaries at which the misorientation between neighbouring measurement points is greater than a defined critical value which depends on the application [10]

3.10
EBSD spatial resolution
minimum distance between two points in different grains (separated by a sharp boundary) that produces two distinctly different EBSPs that can be correctly indexed using an EBSD system

NOTE   An example is shown in Figure 3 where the electron beam has been passed over a boundary in a meteorite specimen. Two distinct and different EBSP orientations can be seen in the far-left and far-right images, but the central EBSP is a mixture of the two. Modern indexing algorithms frequently allow solution of such overlapping patterns, which leads to an effective improvement in the EBSD spatial resolution.
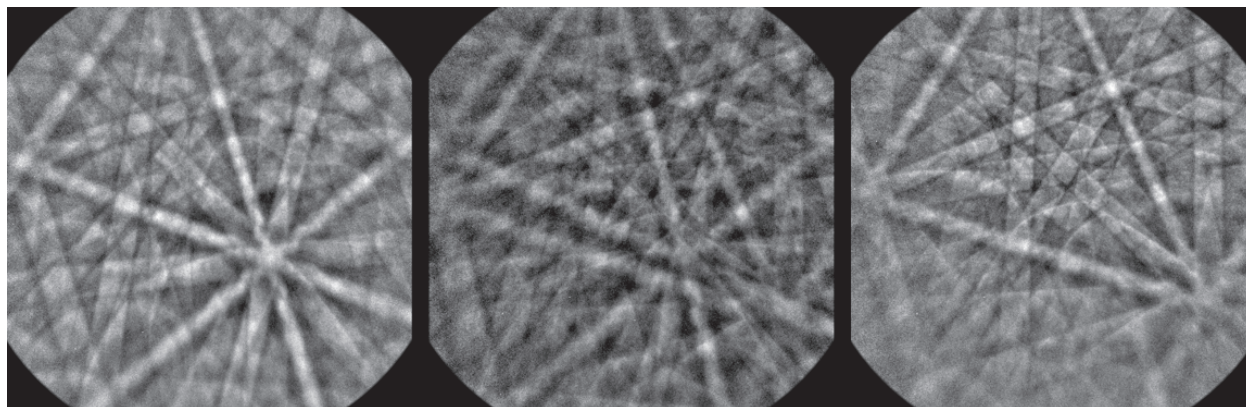
Figure 3 — Examples of EBSPs from either side (far left and far right) and on a grain boundary (centre)
(Note that these images were taken at 30 nm spacings and the centre EBSP is a combination of the other two)

3.11
Euler angles
set of three rotations for representing the orientation of a crystal relative to a set of specimen axes

NOTE   The Bunge convention (rotations about the Z, X′ and Z″ directions) is most commonly used for describing EBSD data. The Euler angles give the rotation needed to bring the specimen coordinate system into coincidence with the crystal coordinate system. It should be noted that there are equivalent sets of Euler angles, depending on crystal symmetry [6].

3.12
Hough transform
mathematical technique of image processing which allows the automated detection of features of a particular shape within an image

NOTE   In EBSD, a linear Hough transform is used to identify the position and orientation of the Kikuchi bands in each EBSP, which enables the EBSP to be indexed. Each Kikuchi band is identified as a maximum in Hough space. The Hough transform is essentially a special case of the Radon transform. Generally, the Hough transform is for binary images, and the Radon transform is for grey-level images [11],[12]. See 5.3.7 for more details.

3.13
indexing
process of identifying the crystallographic orientation corresponding to the features in a given EBSP, for example determining which crystal planes correspond to the detected Kikuchi bands or which crystal directions match the Kikuchi band intersections (zone axes) and thereby determining the orientation (and phase)

3.14
microtexture
population of crystallographic orientations whose individual components are linked to their spatial location within the microstructure [13]

3.15
misorientation
difference in the alignment of the coordinate systems of two crystals, usually expressed as an angle/axis pair

NOTE 1   Misorientation is the rotation required to bring one crystal into coincidence with another. It can be described by a rotation matrix, a set of Euler angles, an axis/angle pair or a Rodriguez vector. The axis/angle pair is most common, but the smallest angle description is generally used.

NOTE 2   The EBSD software calculates the crystal orientation of a particular point on the specimen surface based on the EBSP acquired at that point. The software can then calculate the misorientation between any two chosen acquisition points (which may or may not be neighbours in the orientation map). [14]

3.16
orientation
alignment of a crystal relative to a set of specimen axes

NOTE   It is usually represented by Euler angles (ϕ_1, Φ, ϕ_2) or a 3×3 orientation matrix of direction cosines between the crystal and specimen axes and/or a Rodrigues-Frank vector.

3.17
orientation map
OM
map-like display of crystal orientation data derived from the sequential measurement of the crystal orientation at each point in a grid [15]

NOTE   Alternative terms are crystal orientation map (COM), automated crystal orientation map and orientation imaging microscopy map.

3.18
orientation noise
distribution of orientations resulting from a large number of orientation measurements made within a region of a perfect single crystal

NOTE 1   The region must be small enough that electron beam movement over the region does not cause any detectable change in orientation.

NOTE 2   This distribution is a reflection of the statistical nature of the angular resolution of the EBSD technique.

3.19
pattern centre
PC
point in the plane of the detector screen on a line normal to the plane of the screen and passing through the point where the electron beam strikes the specimen

3.20
phase identification
crystallographic identification of an unknown phase in a specimen by comparing the features of the acquired EBSP with those simulated or calculated from a set of possible candidate phases [16],[17],[18]

NOTE   This can be an automatic process in which the EBSD software searches a preselected set of crystal phase databases and determines the phase whose simulated EBSP best matches the acquired EBSP. In this situation, the procedure is referred to as phase discrimination. Alternatively, it can be a manual process in which features of the EBSP, such as its symmetry, band widths and HOLZ (higher-order Laue zone) lines are used in the identification procedure. In either case, information about the chemical composition obtained using energy-dispersive X-ray spectrometry (EDX) or wavelength-dispersive X-ray spectrometry (WDX) can be additionally used to reduce the list of possible phases, thereby speeding up the process and providing an increased level of confidence in the results.

3.21
phosphor screen
screen used to convert the electron diffraction pattern to a visible light signal which can be detected with a low-light-level camera

NOTE   Most EBSD phosphors are made of a thin layer of phosphor particles, $\approx$ 4 µm to 10 µm in size, held together with a binder and having a final aluminium coating that both dissipates charge and acts as a mirror to increase the EBSP signal but is thin enough to be relatively electron-transparent.

3.22
pseudosymmetry
potential for an EBSP to be ambiguously indexed in several ways due to internal similarities between the EBSPs for certain crystal orientations

NOTE 1   This is a problem with some minerals, e.g. quartz and olivine, and can also occur with some metallic phases.

NOTE 2   A common example is when the <1 1 1> zone in bcc iron is near the centre of the EBSP, as shown in Figure 4. If only the circular region shown is used for band detection, then it is very difficult to distinguish between these two orientations. The <1 1 1> zone has an apparently 6-fold axis, although it really has only 3-fold symmetry, and only weaker Kikuchi bands near the edges of the region can distinguish the two possible 3-fold axes.

NOTE 3   Pseudosymmetry effects can usually be minimized by decreasing the specimen-to-screen distance, in order to capture more Kikuchi bands, and by using more bands for indexing.
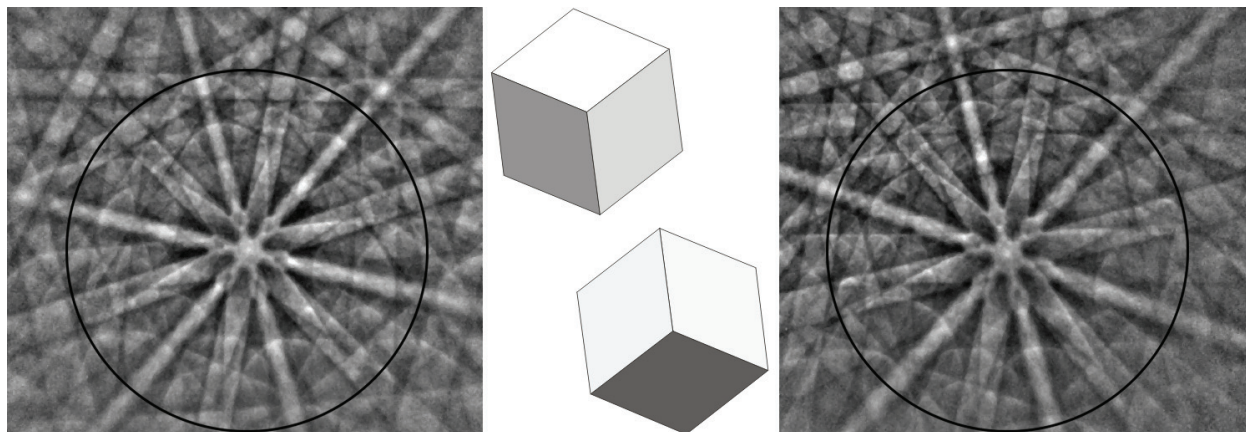
Figure 4 — Pseudosymmetry in bcc iron around a <1 1 1> zone
(If only the stronger Kikuchi bands within the circle are used, then the two EBSPs can be indexed as either of the two orientations shown which are related by a 60° rotation about <1 1 1>)

3.23
specimen-to-screen distance
SSD
distance between the plane of the detector screen and the point where the electron beam strikes the specimen, measured perpendicular to the pattern centre

NOTE   If the specimen-to-screen distance decreases, then the EBSP will appear to zoom out about the pattern centre, i.e. more Kikuchi bands will be seen.

3.24
spherical Kikuchi map
SKM
representation of the EBSP diffraction pattern projected on to the surface of a sphere, as shown in Figure 5, the diffracted signal emanating spherically from a point source on the specimen surface

NOTE 1   Spherical Kikuchi maps are useful in that they avoid the distortions associated with the gnomonic projection of the EBSD signal onto the flat phosphor screen used to capture each EBSP.

NOTE 2   The spherical Kikuchi map is centred about the specimen and aligned with the crystallographic directions of the crystal being examined. As the crystal is rotated, the spherical Kikuchi map moves in synchrony.
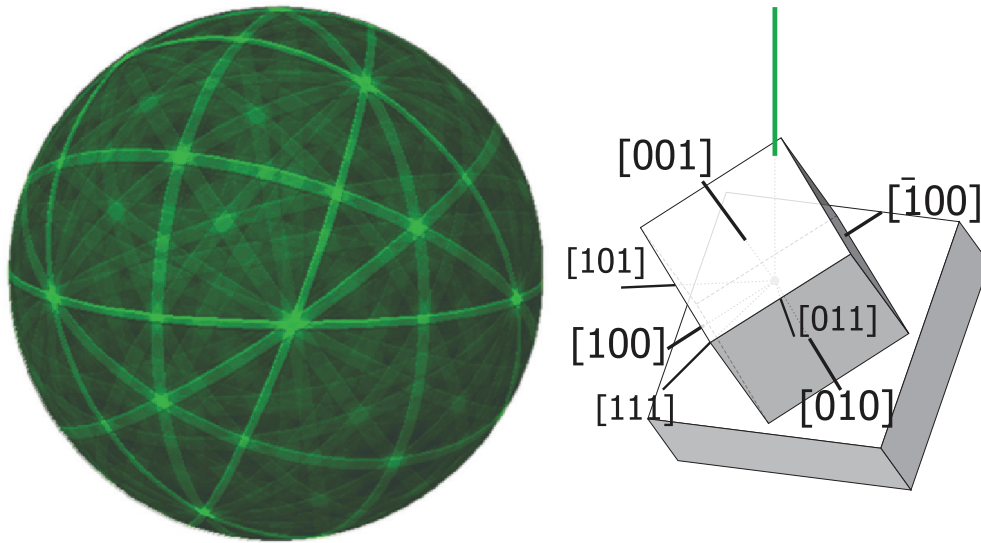
Figure 5 — Schematic diagram showing a silicon unit cell (right) with the main crystal directions labelled and, on the left, a spherical Kikuchi map of silicon at the same orientation
(This orientation is the standard silicon calibration orientation for a 70° tilted specimen;
the incident electron beam direction is shown)

3.25
symmetry
property an object is said to have if it looks the same when rotated, translated or mirrored in a certain way

NOTE   For further information, see Annex C.

3.26
zone axis
point in an EBSP where the centres of several Kikuchi bands intersect

NOTE   It corresponds to a low-index crystal direction in the EBSP.

3.27
Bravais lattice
three-dimensional geometric arrangement of the atoms or molecules or ions making up a crystal

4   Equipment for EBSD

4.1   SEM, EPMA or FIB instrument, fitted with an electron column and including controls for beam position, stage, focus and magnification (see Figure 6).

4.2   Accessories, for detecting and indexing electron backscatter diffraction patterns, including:

4.2.1   Phosphorescent ("phosphor") screen, which is fluoresced by electrons from the specimen to form the diffraction pattern.

4.2.2   Video camera, with low light sensitivity, for viewing the diffraction pattern produced on the screen.

4.2.3   Computer, with image processing, computer-aided pattern indexing, data storage and data processing, and SEM beam (or stage) control to allow mapping.

NOTE 1   Modern systems generally use charge-coupled devices (CCDs).

NOTE 2   Some systems incorporate detector(s) mounted around the phosphor screen to detect electrons scattered in the forward direction from the specimen; the detectors are usually silicon diodes, similar to those used in solid-state backscatter detectors. The images (orientation and atomic number contrast) give a rapid overview of the specimen microstructure [19].

Key
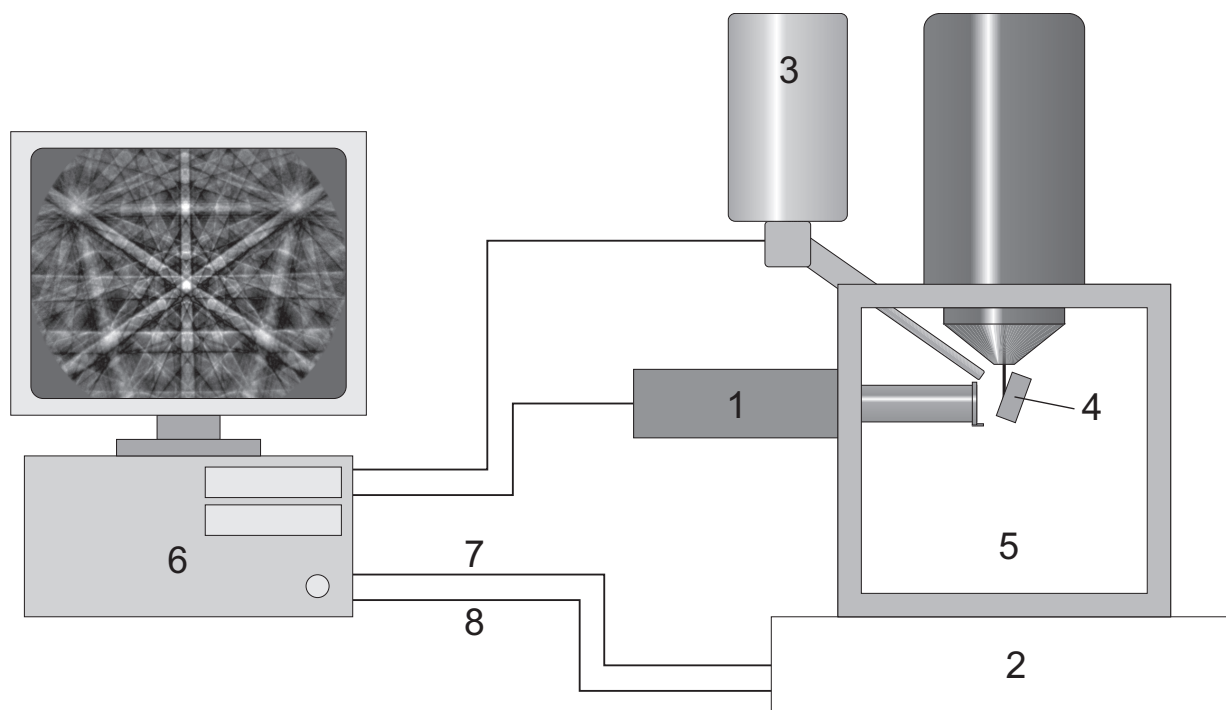
1	EBSD instrument	5	chamber
2	SEM	6	EBSD computer
3	EDX (energy-dispersive spectrometer) (optional)	7	beam control
4	tilted specimen	8	SEM and stage control

Figure 6 — Diagram of an experimental EBSD arrangement

4.3   If specimens need to be prepared for EBSD, the following equipment might be required (depending on the types of specimen to be prepared — see Annex B): cutting and mounting equipment, mechanical grinding and polishing equipment, electrolytic polisher, ultrasonic cleaner, ion-sputtering equipment and coating equipment.

5   Operating conditions

5.1   Specimen preparation

The volume of material sampled by the electron beam during EBSD analysis must be crystalline. The crystal features (e.g. grain size, deformation state) of this volume shall be representative of the bulk specimen or of the part of the specimen about which the nature of the microstructure will be inferred in the case of segmented microstructures (e.g. layered thin films or heat-affected/non-heat-affected zones near welds). Since the EBSP is generated by electron diffraction within a few tens of nanometres of the specimen surface, very good preparation of the specimen surface is required to ensure this and to prevent the EBSD data from being deleteriously affected by inadequate preparation. The top layer under investigation shall be free from deformation due to specimen preparation and flat. Poor specimen preparation can leave deformation at, or just below, the surface or can leave contaminants, oxides or reaction product layers on the specimen surface. Due to the high tilt of the specimen surface (typically 70°) with respect to the electron beam, minimizing

surface relief is also an important part of good specimen preparation. Guidelines on specimen preparation for EBSD are given in Annex B.

5.2 Specimen alignment

Accurate calibration (see Clause 6) and measurement using EBSD requires careful specification of the alignment between the coordinate systems of the specimen, the SEM scanning coils, the stage and the EBSD detector. The specimen shall be aligned in the microscope such that the normal to the acquisition surface is at a chosen tilt angle (typically ≈ 70°) to the electron beam and such that a reference direction on the acquisition surface, often a specimen edge, is parallel to both the stage tilt axis and, in the case of beam scanning, to one axis of the beam-scanning system. Accurate alignment can be achieved more easily when the specimen is mounted on a stage that allows rotation of the specimen within the tilted acquisition plane, since fine adjustment can be performed with the specimen inside the microscope. First, the specimen reference direction shall be aligned with the stage tilt axis. This alignment can be verified by moving the stage back and forth along the tilt axis and checking in the electron image that the specimen reference direction moves back and forth through a fixed point on the display, such as a particular intersection point on a grid overlay. The long axis of the beam scan can then be aligned with the tilt direction by adjusting the scan rotation until these two directions appear aligned in the electron image. If a pre-tilted specimen holder is being used (or the stage does not allow rotation within the acquisition plane), then it is critical that the specimen be mounted with the specimen reference direction as close as possible to one of the orthogonal SEM stage axes.

With a manual-tilt stage, a mechanical end-stop at the desired tilt angle is recommended so that the stage can be tilted to the desired tilt angle with better reproducibility.

5.3 Common steps in collecting an EBSP

5.3.1 Setting the microscope operating conditions

5.3.1.1 Accelerating voltage

To contribute to the formation of the pattern, the electrons must have sufficient energy so that, when backscattered, they retain enough energy to cause scintillation in the phosphor screen. This also increases the number of electrons falling on the screen and thus the brightness of the diffraction pattern. This allows the integration time of the camera to be reduced but will make the spatial resolution poorer by increasing the electron beam size. Note, however, that this reduced resolution is typically only a small effect. An accelerating voltage ranging between 15 kV and 30 kV is recommended for most applications. Increasing the accelerating voltage reduces the electron wavelength and hence reduces the width of the EBSD bands in the diffraction pattern. Higher accelerating voltages within this range are beneficial for analysing the material below a very thin (up to approximately 10 nm) conducting coating or very thin layer of surface deformation. Lower accelerating voltages might be required for analysing thin (10 nm to 50 nm) surface films or to reduce charging on specimens with poor conductivity.

5.3.1.2 Probe current

Increasing the probe current will increase the number of electrons contributing to the diffraction pattern and so allow the camera integration time to be reduced, allowing faster mapping. However, this advantage must be balanced against the associated loss of spatial resolution because increasing the probe current results in the EBSD signal being generated from a larger volume in the specimen and also increases problems due to both charging and contamination effects.

The electron beam shall be focussed on the specimen surface and dynamic focussing used, if available, to compensate for the tilted specimen.

5.3.2 Detector and working distances

For general use, the ideal working distance for EBSD is the working distance at which the brightest region of the raw EBSP (i.e. without background correction) is in the centre of the phosphor screen. Other experiments can dictate a different position. Pattern intensity can be increased by increasing the camera gain but at the

expense of increasing noise levels. Short working distances will generally improve the spatial resolution of EBSD measurements, although additional care has to be taken to avoid collisions between the specimen and the pole-piece or the backscatter detector (if present).

The ideal detector (specimen-to-screen) distance for EBSD depends on the size of the phosphor screen and on the nature of the analysis being conducted. For a typical EBSD investigation, the phosphor screen is placed approximately 15 mm to 25 mm from the point of intersection between the electron beam and the specimen. With a smaller specimen-to-screen distance, more bands are captured in each EBSP, which can be useful for improving the indexing of low-symmetry phases and for improving discrimination between phases or of orientations with similar (pseudosymmetric) EBSPs. With a larger specimen-to-screen distance, a smaller region of diffraction space is imaged on the phosphor screen, and the bands in each captured EBSP are wider. Automated indexing might, however, not be possible if the detector distance is increased beyond a certain value.

At low magnifications, the pattern centre position will move significantly during beam scanning, and this will affect the accuracy of the orientation data collected. Some systems have calibration and indexing routines that account for this movement. Some systems allow for calibrations at different working distances and interpolate between these for intermediate working distances. The range of working distances for which the EBSD system remains accurately calibrated shall be determined.

5.3.3   Camera integration/exposure time

Most modern CCD cameras have the ability to control the amount of time that the camera pixels are exposed to light. This parameter is usually referred to as the camera integration or exposure time. Long exposure times will generally give better-quality EBSPs with lower noise levels; however, if the exposure time is too long, parts of the image can become saturated (i.e. completely white).

The integration time should be set so that the raw EBSP (i.e. without background correction) is as bright as possible without any portion of the EBSP becoming over-saturated. The integration time required to achieve this condition will be smaller with higher atomic number of the phase being examined, higher accelerating voltage, higher probe current, smaller detector distance, lower camera resolution (higher binning levels) and higher gain setting. The integration time shall be optimized for the specific conditions used in each experiment to make full use of the dynamic range of the CCD. A useful check is to examine the grey-level histogram of the raw, unprocessed EBSP and to adjust the settings so that approximately 75 % of the range is being used.

5.3.4   Binning

Most modern CCD cameras are capable of combining blocks of pixels to give an enhanced, i.e. brighter, signal and higher camera sensitivity, at the cost, however, of a lower-resolution image. Binning can be used to increase the speed of EBSP mapping as the increased binning results in a faster CCD readout speed. Binning also increases the effective sensitivity of the detector.

The series of images in Figure 7 shows the effects of binning on the EBSP signal and speed as the binning factor is repeatedly doubled. Each doubling corresponds to a halving of the EBSP image width in pixel units.
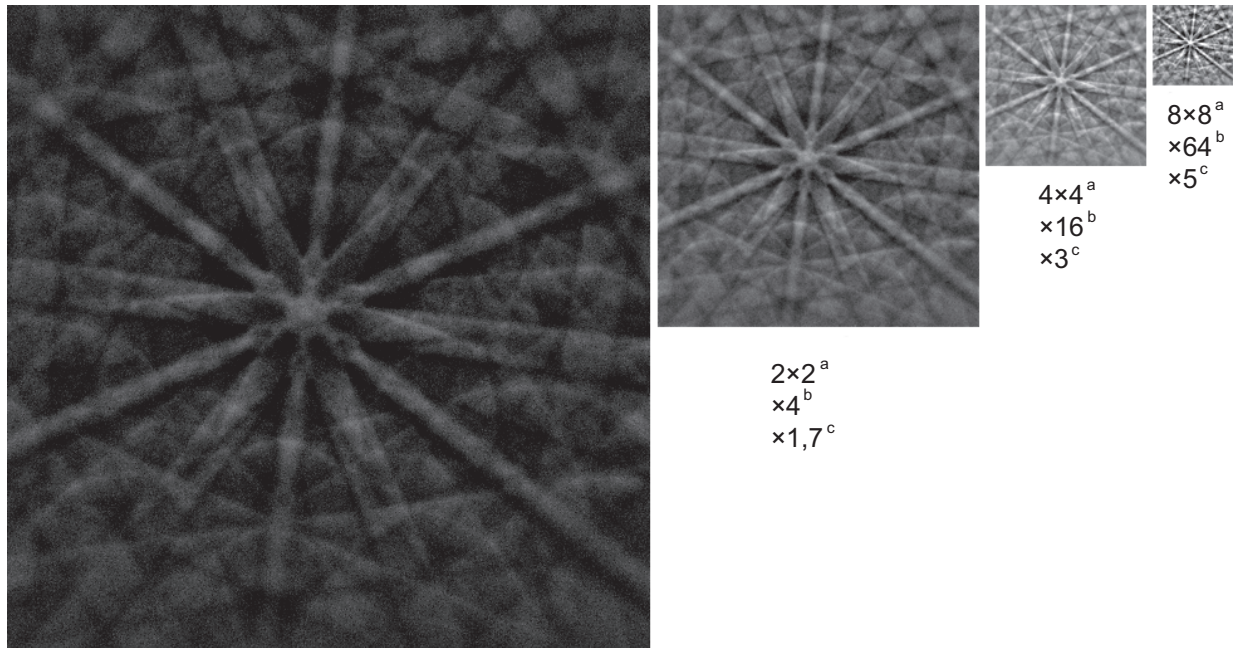
a   Binning.

b   Image intensity (compared to that obtained without binning).

c   Readout speed (compared to that obtained without binning).

Figure 7 — Schematic diagram showing the effect of camera binning on image size, intensity and speed

5.3.5   EBSP averaging

Digital averaging of several EBSPs gathered from the same crystal volume is sometimes carried out to reduce the noise level in the final EBSP. EBSP averaging leads to higher-quality EBSPs but slows down the EBSD mapping speed. The total camera time is the product of the camera integration time (time per frame) and the number of frames used to obtain the averaged EBSP but can improve indexing rates and indexing quality in some applications. Averaging between 1 frame (i.e. no averaging) and 3 frames is typical for mapping. Higher levels of averaging can be used for some applications, such as difficult phase identification.

5.3.6   EBSP background correction/EBSP signal correction

EBSPs generally have a bright centre and become much darker near the corners. Background correction should be used to convert the "raw" EBSPs into ones with more uniform average brightness across them and with better local contrast near the edges and corners. Background correction involves collecting a background signal and then removing it from an EBSP by subtraction, division or a mixture of the two. (Division usually improves the contrast in the corners of the EBSP and, in image-processing terms, is called "flat-fielding".)

Two methods are generally used to obtain a signal for the background correction. In the first method, an EBSP is collected while the beam is scanned over a large number of grains in a polycrystalline specimen. Since a large number of EBSPs has been averaged, the resulting pattern has no bands but retains the brightness gradient from centre to corners that is present in raw EBSPs. This pattern with no bands is used as a background to enhance the contrast in all subsequently collected EBSPs. In the second method, a background is created from each collected EBSP by using a mathematical "blurring" function to smooth out the short-range contrast (i.e. the bands). This background is then used to enhance the contrast in the EBSP from which it was created. This method tends to accentuate flaws in the scintillator (phosphor) or abnormal pixels in the CCD, so its use should be avoided on a system with these problems. The time taken for pattern processing is also slightly greater when using this method.

For many applications, particularly the analysis of deformed materials, it is advisable to use a combination of both methods. For some applications, one method can be preferable. The second method is very useful for single-crystal specimens and for specimens with very large grain sizes, where it can be difficult or impossible to scan the beam over a sufficiently large number of grains. If the first method is used for such specimens, the specimen should, if possible, be continuously rotated while the background is being acquired; this will smear out the EBSP and produce a better background than digital smoothing of the EBSP.

5.3.7 Band detection

Band detection during EBSD refers to the automatic detection of Kikuchi bands in an EBSP via use of a Hough transform, as depicted below [11],[12].

Note the following:

a) At the user's discretion, the resolution of the EBSP can be reduced by binning, to increase speed.

b) Hough space is parameterized in terms of ρ and θ which represent the distance of each specimen line from the origin and the inclination of the line, respectively (see Figure 8). A point in Hough space transforms to a straight line in the EBSP. Correspondingly, a point in each EBSP transforms to a sinusoidal curve in Hough space that defines each specimen line that passes through the point.

c) Once the Hough space transformation has been carried out (in practice, this is achieved using an accumulation algorithm) and, optionally, normalized (to correct for the variation of specimen line length with position in Hough space), the Hough image can be filtered to highlight the peaks that correspond to the Kikuchi band. This is normally done using a so-called "butterfly" filter. In Hough space, each Kikuchi band appears as a bright peak with a pair of darker valleys above and below. The bright peak corresponds to the Kikuchi band centre, and the dark valleys to the two edges of the Kikuchi band.

d) The Kikuchi bands detected can optionally be displayed on top of the original EBSP.

e) The quality of indexing for given settings of the Hough transform shall be checked (see Clause 8). If the indexing is poor, the suitability of the settings for the Hough transform should be investigated.

Care is required in setting the parameters for the Hough transform, and the effects of changing them on the indexing of patterns of materials similar to those of interest should be observed.
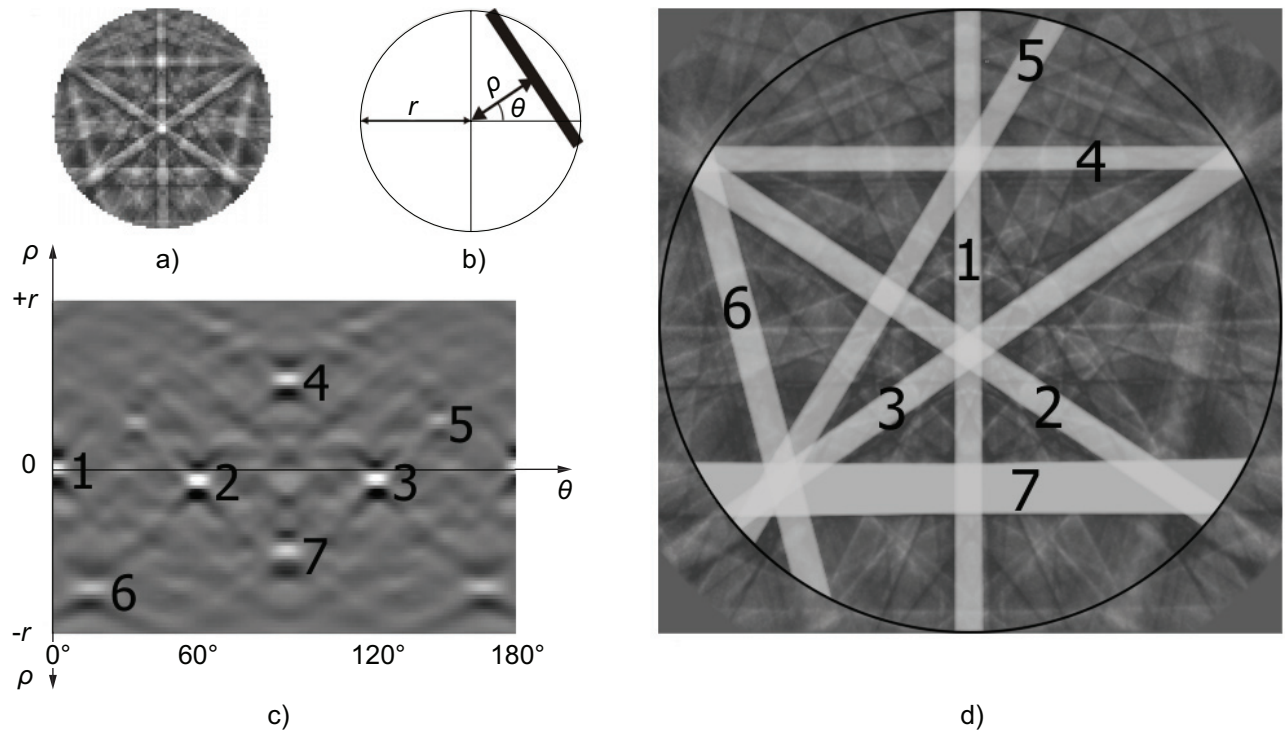
Key

r   radius of area of interest

ρ   distance of a specimen line from the origin

θ   inclination of the specimen line

Figure 8 — Schematic diagram showing a) a downsized EBSP of ≈ 100 pixels in width; b) a Hough space parametrization; c) a Hough transform of the EBSP shown in a); d) the original EBSP with the detected bands 1 to 7, corresponding to the numbered peaks in c), superposed

6   Calibrations required for indexing of EBSPs

6.1   Calibration of the EBSD system geometry is required to measure accurately the relationship between the specimen and the crystallographic axes (the crystal orientation). For this, it is necessary to be able to determine the (x, y) position of the pattern centre (PC) on the phosphor screen and the specimen-to-screen distance (SSD) (see Figure 9).

6.2   The calibration applies to a fixed tilt angle of the specimen, a fixed position of the screen or camera assembly and a fixed working distance of the microscope. Any alteration of any of these parameters can affect the result of pattern indexing and requires a recalibration.

In systems where magnetic fields are present near the specimen, calibration shall also include measurement of the effects of distortions in the EBSP caused by these magnetic fields.

6.3   At any magnification, the PC position will move as the beam is scanned over the specimen. At low magnification, the PC motion can be significant and might affect the accuracy and results of the indexing routines. Some systems have calibration and indexing routines that allow for this movement. Some systems allow calibration at different working distances and interpolation for intermediate working distances. It is important that the range of working distances for which the EBSD system remains accurately calibrated be known.

6.4   The EBSP is a gnomonic projection of the diffraction sphere on to the detector screen; points furthest from the PC are distorted/stretched the most. The PC and the SSD are the most important calibration parameters and, for accurate absolute orientation measurements, the PC shall be accurately determined.
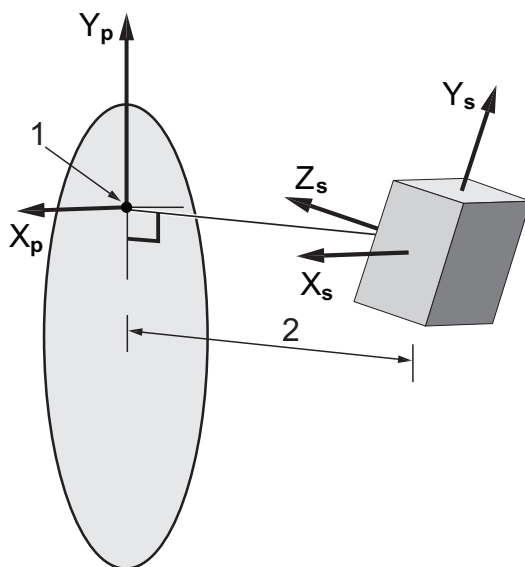
Key

1   pattern centre (PC)

2   specimen-to-screen distance (SSD)

Figure 9 — Schematic diagram showing the main EBSD geometry calibration parameters

6.5   If the PC is displaced, then the centre of the EBSP diffraction sphere will also be displaced by the same amount. For small displacements, this will appear in certain parts of each pattern to be a rotation, hence it can be difficult to accurately fit the PC position using iterative fitting of the Kikuchi bands.

NOTE   The images in Figure 10 show a silicon EBSP a) correctly calibrated (note how well the simulated black lines match the Kikuchi bands), b) with the PC displaced horizontally and c) with the PC displaced vertically.
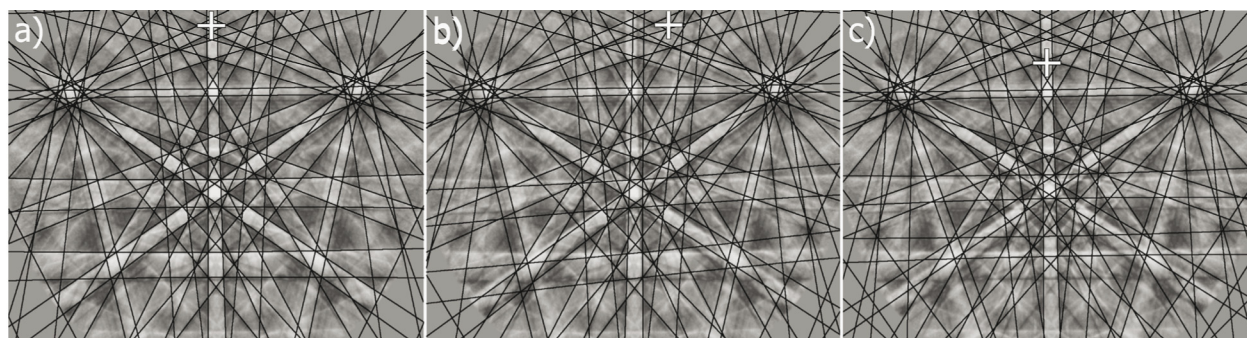
Figure 10 — Example of EBSP indexing as a function of PC position: a) correct indexing with an accurate PC (white cross) — the simulated bands (black) align with the real Kikuchi bands; b) the PC is displaced horizontally and c) vertically, resulting in obvious errors in the simulated band positions

6.6   The following four methods of calibration are used to determine the PC and SSD:

a)   **Iterative pattern fitting:** In this method, approximate values of the PC coordinates and the SSD are used as the starting values for a fitting (parameter refinement) procedure between the Kikuchi line positions in an EBSP collected from a known material (commonly the specimen under investigation) and the simulated Kikuchi line positions for a given crystal orientation. This is the most common method in use with commercial systems. By repeating the calibration on several EBSPs and averaging the results, a more accurate calibration can be achieved.

It is important that the known phase be accurately represented in the database.

b)   **Shadow-casting techniques:** These are rarely used now but have a place in precision work [2].

c)   **Use of a crystal of known phase and orientation:** Single crystals of germanium, silicon or nickel are commonly used. The crystal shall produce high-quality EBSD patterns and the plane parallel to the acquisition plane and the direction parallel to the tilt axis shall be known. The accuracy of the calibration (and therefore the accuracy of absolute orientation measurement using the EBSD system) depends on the accuracy with which these planes and directions are known. Therefore, it is recommended that these planes and directions be known to within an accuracy of 0,5°.

An example of an indexed silicon EBSP is shown in Figure 11.
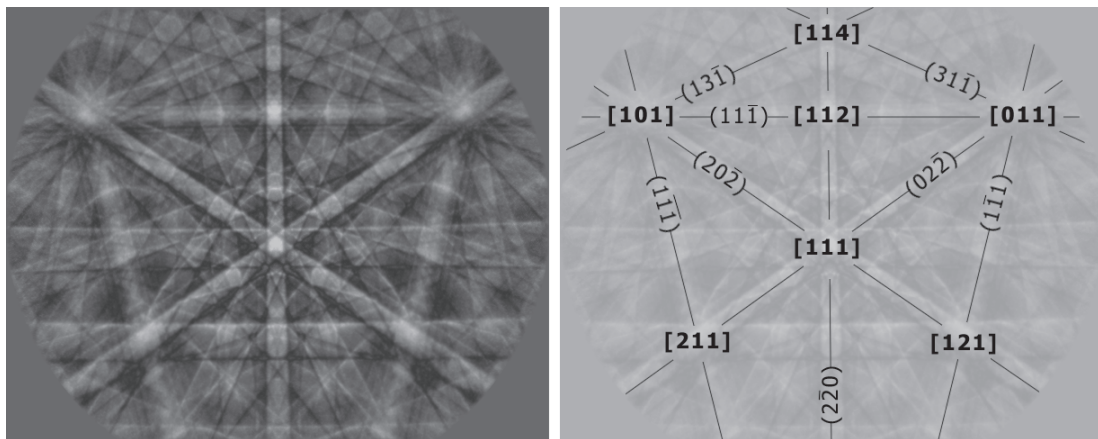

Figure 11 — Example of a silicon EBSP (left) with the main planes and zones labelled (right)

A common material for this purpose is polished Si cut on the (0 0 1) plane, with the edge of the calibration crystal cut along <1 1 0>, which should be aligned accurately with the stage tilt axis. For a detector with a vertical screen and a 70,53°-tilted silicon specimen, the PC lies in the [1 1 4] zone, and the SSD can be determined by measuring the distance between two known zone axes, e.g. [0 1 1] and [1 0 1], and relating the distance in pixels to the known angle between the two zone axes, which is 60° in the case cited. For a number of reasons, this is often used to locate the approximate SSD and PC, and the iterative method is used to refine the values.

It is better to mount the reference single crystal together with the specimen to be investigated at the same tilt, typically 65° to 70°. There should be a reliable and accurate means of aligning the specimen axes with the microscope frame to obtain reproducible EBSD measurements (and not only to calibrate the SSD). If the calibration is not further defined for the specimen to be investigated, then the same accelerating voltage, working distance, tilt angle and detector distance values should be used as were used for the calibration, i.e. the specimen should be moved to the operating position using only stage movement to avoid changes to the beam focus.

If the calibration is refined using a pattern from a known phase in the material to be measured [see 6.6 a)], then small deviations from the working conditions used to generate the calibration data are permissible.

NOTE   For high-symmetry materials, there will always be several possible positions for detection that would give the same EBSP. This is shown in Figure 12 where the EBSD detector is looking at the highlighted "kite" but could equally well be looking at any of the other highlighted equivalents.
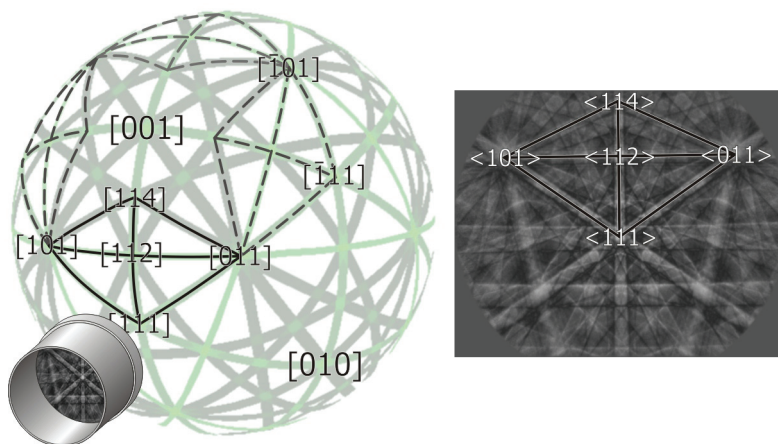
Figure 12 — Schematic diagram showing how a calibration EBSP (right, with a "kite" labelled) can be misinterpreted when used to calibrate an EBSD detector. There are several possible viewpoints for the EBSD detector that would produce the same EBSP (as shown by labelled "kites" on the left). Miscalibration of this kind will result in consistently rotated, incorrect orientation data.

d) **Pattern magnification:** In this method, an EBSP is taken with the detector fully inserted and another with the detector partially retracted. The EBSP will thus zoom about the PC, and the (x, y) coordinates of the PC can be located by comparing similar features in both EBSPs (see Figure 13). The SSD is determined as in method 6.6 a) in the working position.
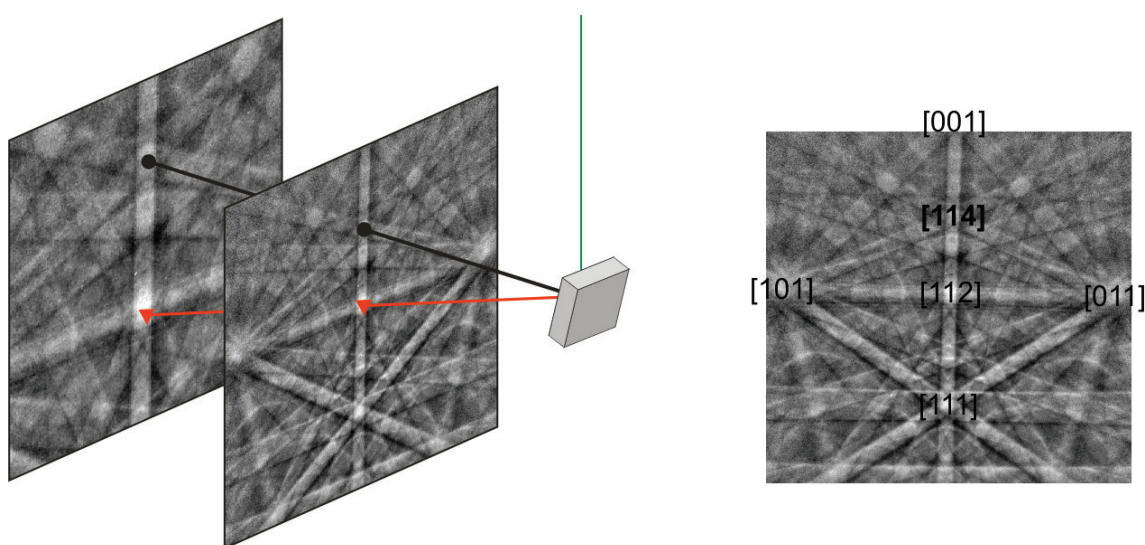
Figure 13 — PC calibration by the moving phosphor method. By moving the EBSD detector, the EBSP will appear to zoom out/in about the PC. This is shown schematically on the left. The indexed EBSP is shown on the right. In this case, the pattern centre is the [1 1 4] zone axis.

7   Analytical procedure

7.1   Pre-test preparation

Before the specimen is observed under the electron microscope, it is useful to mark the position of the area of interest. Micro-hardness indents can be used for this purpose. Note that micro-hardness indents can be difficult to find with the SEM, so they should be complemented either by macro-hardness indents (placed at sufficient distance to avoid introducing plastic deformation into the area of interest) or by the use of a marker

pen (this method is very efficient and convenient, but the marks can be removed if the specimen is later rinsed with ethanol or a similar solvent). If the axes of the specimen coordinate system are not defined by the edges of the specimen or by other easily recognizable features on the specimen, then they should be marked. For this purpose, indentations or a marker pen can be used or, alternatively, lines can be scribed on the specimen surface, again taking care to place the lines sufficiently far from the area of interest.

7.2 Operating conditions

The operating conditions shall be determined as described in Clause 5.

7.3 Equipment stability check

Some hours after starting the equipment, and again during use, the stability of the system should be verified.

With most FEG-SEMs, at extremely high magnification and with very small EBSD map step-size ($\approx$ 50 nm or below), it is recommended that several hours be allowed for stabilization. The electron gun stability and probe current stability are important parameters and should also be monitored during collection of EBSD data. Sometimes, stage drift can occur, and it should therefore be checked. It is recommended that a recording of the image before and after map acquisition be made to detect whether the specimen moved.

7.4 EBSD analysis

Once the above steps have been carried out, EBSD analysis can be performed on the specimen. The analysis cycle consists of beam positioning, EBSP acquisition, band detection, indexing and saving of the data. This cycle shall be repeated for each data point.

NOTE   While it is common both to capture and to index the EBSP for each point during the acquisition cycle, it might be possible to capture and save the EBSPs, or the position of peaks in Hough space, depending on the system being used. Saving the data can also be done concurrently with indexing, if desired. Retrieval of the EBSPs or the Hough peaks (depending on what is saved), followed by band detection, indexing and saving of the results, is carried out at a later time. This allows varying degrees of parameter adjustment during the indexing process.

8 Measurement uncertainty

8.1 General

Though this International Standard is only concerned with the measurement of absolute and relative orientation using EBSD, all measurements are associated with a certain level of uncertainty, and it is important that the user be aware of the factors that can influence the measurement results from an early stage.

The acceptable level of uncertainty in an EBSD measurement and the requirements for achieving this depend on the type of EBSD analysis being conducted, the material being analysed and the purpose for which the result will be used. The contribution of measurement uncertainty to the qualification and quantification of EBSD results should be considered in the contexts discussed in 8.2 to 8.4.

8.2 Uncertainty of crystal orientation measurement

The uncertainty of the crystal orientation measurement by EBSD is a combination of the following factors:

a) uncertainty in the specification of the specimen coordinate system;

b) uncertainty in the specification of the alignment between the specimen coordinate system and the coordinate system of the EBSD detector;

c) uncertainty in acquiring the EBSP;

d) uncertainties in the band detection and the indexing of the EBSP;

e) the equipment and instrument operating settings (accelerating voltage, spot size, beam current, working distance, etc.).

8.3 Absolute orientation

The crystal orientation is measured with respect to the specimen coordinate system. Results will be affected by all factors listed in 8.2.

8.4 Relative orientation

The orientation of one crystal is measured with respect to another (i.e. the misorientation between two crystals is measured). This is independent of the uncertainty in the specification of the specimen coordinate system and the uncertainty in the specification of the alignment between the specimen coordinate system and the coordinate system of the EBSD detector, except for the uncertainty associated with the adjustment of the EBSD system calibration to allow for the resulting change in geometry between the point of beam impingement and the detector screen (dynamic calibration). The measurement of relative orientation will also not be affected by any components of the uncertainties that are systematic (i.e. do not vary from point to point or orientation to orientation) but only by those components that do vary from point to point or orientation to orientation.

If a specimen contains more than one phase and these phases have different Bravais lattices then, in general, EBSD can be used to distinguish correctly between the different phases by matching the interplanar angles between theoretical and experimental results. For materials where pseudosymmetric patterns are expected, or which have very similar EBSPs, EDX (energy-dispersive X-ray spectrometry)/WDX (wave-dispersive X-ray spectrometry) data can be used to help distinguish between different phases. Alternatively, in cases where more than one phase present has the same Bravais lattice, the Kikuchi bandwidth measurements can also be used to distinguish between the phases.

It is the responsibility of the user to record the equipment and acquisition parameters (see 9.3), and to calculate the type A and type B uncertainties for the laboratory's set-up in accordance with ISO/IEC Guide 98-3. Detailed guidelines on classifying uncertainty contributors and then estimating the uncertainty in the wide variety of measurements that can be derived from EBSD data fall outside the scope of this International Standard but might be covered in future International Standards relating to the various applications of EBSD.

9 Reporting the results

9.1   The results of the analysis shall be reported in accordance with the requirements of ISO/IEC 17025.

9.2   The specimen preparation method and the section of the specimen analysed shall be clearly indicated.

9.3   The SEM and EBSD operating conditions shall be indicated. Indicate gun type, accelerating voltage, working distance, probe current (if available), specimen tilt angle and type of scan (beam or stage), step size and magnification (or image width).

9.4   In presenting the data, include at least one map showing the "raw" data (prior to any data-cleaning operations) to allow the reader to check for artefacts due to data-cleaning procedures.

Annex A
(informative)

Principle of EBSD

When an electron beam is focussed on a tilted crystalline specimen, a divergent source of electrons is generated within the specimen by inelastic scattering involving little energy loss. Electrons from the source that are incident on a set of crystal planes at an angle that satisfies the Bragg equation ($2d\sin\theta = n\lambda$) are diffracted (θ being the angle of incidence of the incident beam, d the interplanar spacing, λ the wavelength of the incident beam and n an integer). For a family of atomic-lattice planes, the electron backscatter diffraction results in a set of two cones of diffracted electrons as shown in Figure A.1. For the acceleration voltage considered (typically 20 kV), the Bragg angles are about 1°, so the cones of diffracted electrons are largely opened and nearly parallel to the diffracting plane. The intersection of these cones with the phosphor screen placed in front of the specimen leads to the formation of a pair of thin lines. These are called Kikuchi lines and define an EBSD band, the trace of the diffracting plane lying between the pair of lines at an equal angle to each. The resulting electron diffraction pattern consists of many Kikuchi bands, each band corresponding to a family of diffracting planes. According to the Bragg equation, the Kikuchi line spacing, for a given value of λ which can be determined by the accelerating voltage of the electron beam, is proportional to the Bragg angle θ, when θ is small enough, and inversely proportional to the interplanar spacing. The intersections of the Kikuchi line pairs correspond to zone axes in the crystal, i.e. crystallographic directions. In addition, many electrons are inelastically scattered and contribute to the formation of a diffuse background in the pattern.
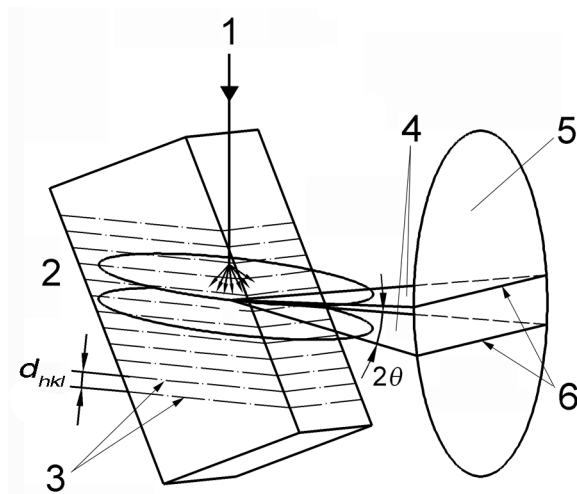
Key

1   incident electron beam
2   tilted specimen
3   lattice planes ($h\,k\,l$)
4   Kossel cones
5   phosphor screen
6   Kikuchi lines

Figure A.1 — Mechanism for the formation of the Kikuchi bands for a given set of crystal planes

Annex B
(normative)

Specimen preparation for EBSD

NOTE   Clauses B.1 to B.7 and Figures B.1 to B.4 have been adapted, with permission of Oxford Instruments, from the section "Sample Preparation for EBSD" on the Oxford Instruments Electron Backscatter Diffraction website.

B.1 General

Because diffracted electrons escape from within only a few tens of nanometres of the specimen surface, any surface defects, such as surface deformation, and surface contaminants and oxide or reaction product layers will influence the electron diffraction signal, resulting in EBSPs of either low quality or spurious origin. To avoid this, careful preparation is needed for most bulk specimens to obtain useable EBSPs. Some specimens, however, such as crystal films or planar cleavage surfaces with low levels of surface relief, require no preparation prior to analysis. Each material under investigation should be considered on an individual basis, and the preparation scheme should be chosen appropriately. More details can be found in ASTM E 3 [20] and ASTM E 1558 [21].

B.2 Cutting

B.2.1   When cutting specimens for EBSD, the orientation of the specimen axes shall be preserved and recorded. For rolled sheets, the significant specimen directions (rolling direction, transverse direction and specimen normal direction) shall all be recorded.

B.2.2   The cutting process shall not damage or change the specimen as this will lead to erroneous results. Avoid aggressive cutting methods that generate heat or cause deformation at the cut surface. Severe damage induced at this stage may extend so deep into the material that it is not removed by subsequent grinding and polishing. Heating caused during cutting may cause changes to the microstructure — phase transformations, recrystallization or precipitation/diffusion may take place. Therefore, heating shall be avoided.

B.3 Mounting

Small specimens generally require mounting so that the specimen is supported in a stable medium for grinding and polishing. The medium chosen can be either a cold-curing resin or a hot-mounting compound.

Mounting is needed for polishing, but the mounting could be removed after polishing to prevent charging effects. A conductive mounting material is preferred for EBSD analysis as it helps to minimize electron beam charging effects which can cause intensity blooming in the EBSD patterns and image drift and distortion in orientation maps. Often, even non-conductive specimens can be mounted in such materials and observed using EBSD without requiring a conductive coating. If the specimens cannot withstand the heat/pressure required for hot mounting, then the use of other mounting materials may be necessary. For example, ceramics are often very brittle and cannot be subjected to pressure without fracturing. In this case, a cold-mounting epoxy may be more appropriate. Before analysis, the non-conductive surface of the epoxy may be painted with conductive silver or carbon paint to minimize charging effects.

B.4 Grinding

B.4.1   Grinding can be carried out in a number of ways, using a variety of abrasives. Fixed abrasive surfaces are available using SiC, Al_2O_3, diamond or cubic nitride abrasives. Grinding on a surface that has blunt abrasives causes a great deal of surface damage by smearing, "burnishing" and local heating. Damage introduced during grinding can be invisible in the polished surface, but can serve to distort the EBSD result or

even completely suppress pattern formation. Therefore, in order to maintain sharp abrasive particles, grinding papers should be changed frequently during the specimen preparation process. Also, the selection of grinding material and conditions should be specific for a given specimen.

B.4.2   After every grinding stage, it is advisable to inspect the ground surface using a light microscope in order to ensure that all damage from the previous stage, whether it was a cutting or grinding stage, has been completely removed. Progress in this manner to the finest abrasive size required for the specimen to be ready for polishing.

B.5 Polishing

B.5.1   It is usually the case that polishing is started on a hard cloth with a coarser abrasive and finished on a softer cloth with a finer abrasive. Final polishing should not be prolonged, but just sufficient to achieve the desired surface finish without causing excessive relief. Extreme undulation or relief in the polished surface should be avoided.

Diamond polishing compounds or slurries are good for the preliminary stages for most materials. Typically, diamond polishing is carried out down to a 1 µm or 0,25 µm particle size, and this is followed by polishing with a 0,05 µm colloidal-silica slurry. A polishing time for this final step of between a few minutes and about 20 min is common for metals, while geological specimens or ceramics may require hours. Harder polishing surfaces or cloths produce a flatter, i.e. more nearly plane, surface, but can leave polishing damage at the surface of the material, such as superficial scratching.

B.5.2   For EBSD of geological or ceramic specimens, it is generally necessary to use an additional final polishing stage using colloidal silica for a minimum of 10 min. This procedure can also produce better results for metal specimens having hard second phases, such as carbide. Colloidal silica is a chemo-mechanical polish, i.e. it combines the effect of mechanical polishing with etching. This type of stock removal is ideal in many cases for EBSD, as a damage-free surface can be obtained with little effort. Figure B.1 shows the effect of chemo-mechanical polishing. Note that the film which forms on the polished surface during polishing must be removed. A convenient method to achieve this is to flush the polishing wheel with water during the last few seconds of polishing, thereby cleaning the specimen surface. The specimen is then removed and dried in the usual manner, using a solvent which has a low water content and is not so volatile as to cause water condensation on the surface. In some cases, 0,5 % to 1 % hydrochloric acid or nital (a mixture of alcohol and nitric acid) can be used to further clean the residual colloidal silica from the specimen surface.
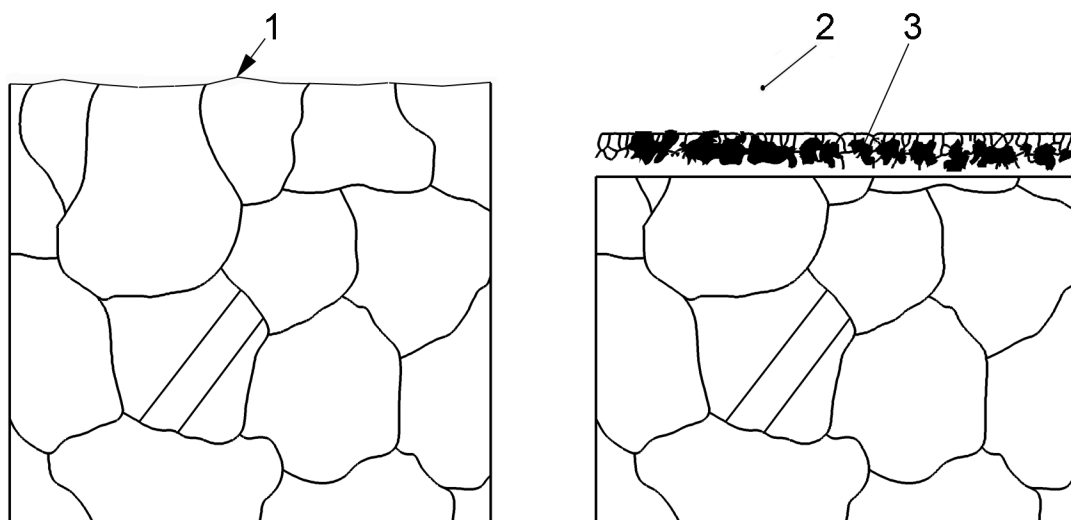
Key

1   residual surface damage

2   surface layer removed by chemo-mechanical polishing with 0,05 µm colloidal silica or oxide

3   film formed during polishing (also removed)

Figure B.1 — Removal of residual surface damage by chemo-mechanical polishing

Flush the polishing wheel with water until all traces of colloidal silica have been washed away, spin to dry and store in a suitable container in which contamination of the wheel cannot occur. Meticulous attention to avoiding contamination of polishing wheels is an important aspect in achieving the best results. The use of colloidal silica produces good results with nearly all materials, and is particularly effective with ceramic and geological specimens that are otherwise difficult to prepare.

B.6 Etching

B.6.1 Polished surfaces can be examined using EBSD, but in many cases the pattern quality is improved by etching. Additionally, etching delineates the grain structure, which is of obvious benefit. However, etching may attack a second phase preferentially or attack grain boundaries excessively. Materials that are difficult to polish may benefit from repeated etching and repolishing. This method can expose an undamaged surface suitable for EBSD when conventional polishing and etching fail to achieve an adequate surface. Any etchant that is used shall dissolve the specimen surface in an even manner and not leave behind any oxide or reaction product layers. Such layers can completely suppress diffraction. Many etchants listed in metallographic textbooks are "contrast etches" which rely on the formation of oxide layers of different thicknesses to generate colours which are visible when using a light microscope. Such etches are generally not suitable for EBSD.

B.6.2 Electrolytic polishing and etching are effective methods for dissolving the deformed layer near the surface of a metal specimen by applying a controlled voltage for a controlled time to the specimen in an electrolytic cell. Figure B.2 shows the characteristic curve for an electrolytic cell. This curve is dependent on the electrolyte used and will vary for different electrolytes. Control of the voltage and current density at the anode, plus electrolyte composition, temperature and stirring, are all critical in achieving the desired etching/polishing characteristics.
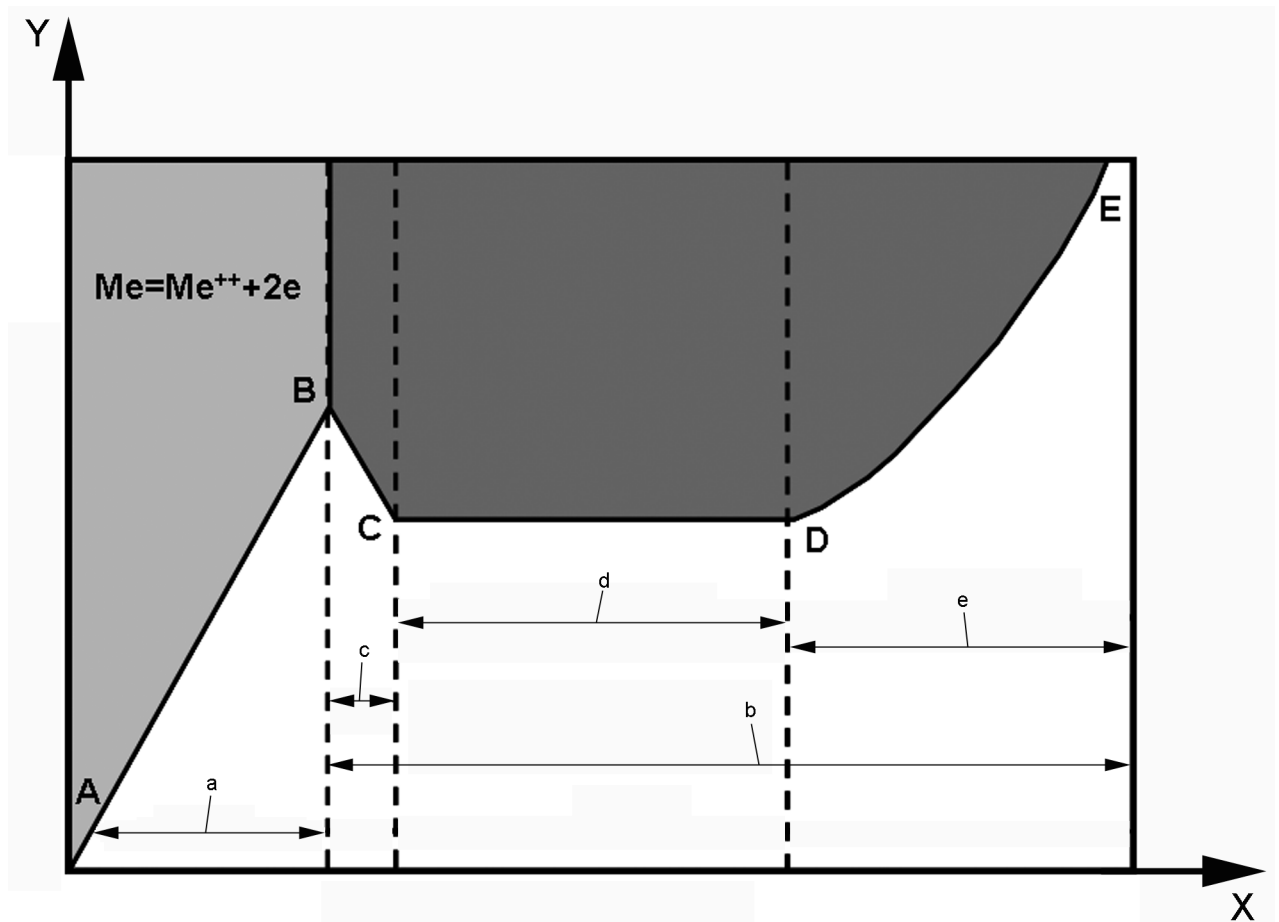
Key

X   voltage

Y   current density

a   Etching.

b   Polishing.

c   Formation of viscous electrolyte layer.

d   Best polishing.

e   Oxygen formation.

Figure B.2 — Characteristic curve for an electrolytic cell

B.6.3   Plasma etching is a process which is the reverse of sputter coating. Generally, it should be used as a means of cleaning or improving a mechanically or electrolytically prepared surface.

B.7 Ion beam techniques

B.7.1   Ion milling is a process, applied to a specimen under vacuum, whereby a selected area of the surface is bombarded by an energetic beam of ions. Generally, the use of rotation and grazing bombardment angles promotes even erosion of the specimen surface and minimizes damage effects. However, certain grain orientations, grain boundaries and phases can erode at different rates, as shown in Figure B.3. Ion milling can give reasonably high rates of material removal, and this can be enhanced by the use of reactive gases, such as iodine, in the reaction chamber. The EBSD pattern quality is determined by the milling time, as shown in Figure B.4. Ion milling can produce surfaces suitable for EBSD with minimal prior preparation, especially with materials that are difficult to prepare by conventional metallography, such as zirconium and zircaloys.

a) **Mechanically prepared surface**   b) **Ion-milled surface**
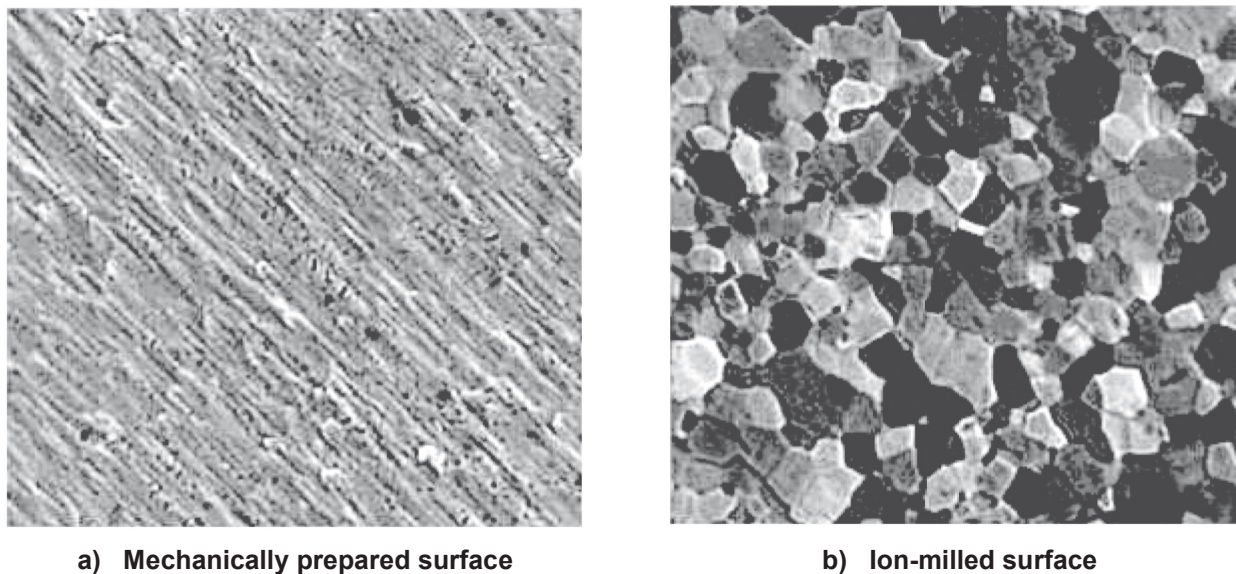
Figure B.3 — Effect of ion milling on titanium [back-scattered electron (BSE) images]

a) **No ion milling**   b) **5 min**   c) **15 min**
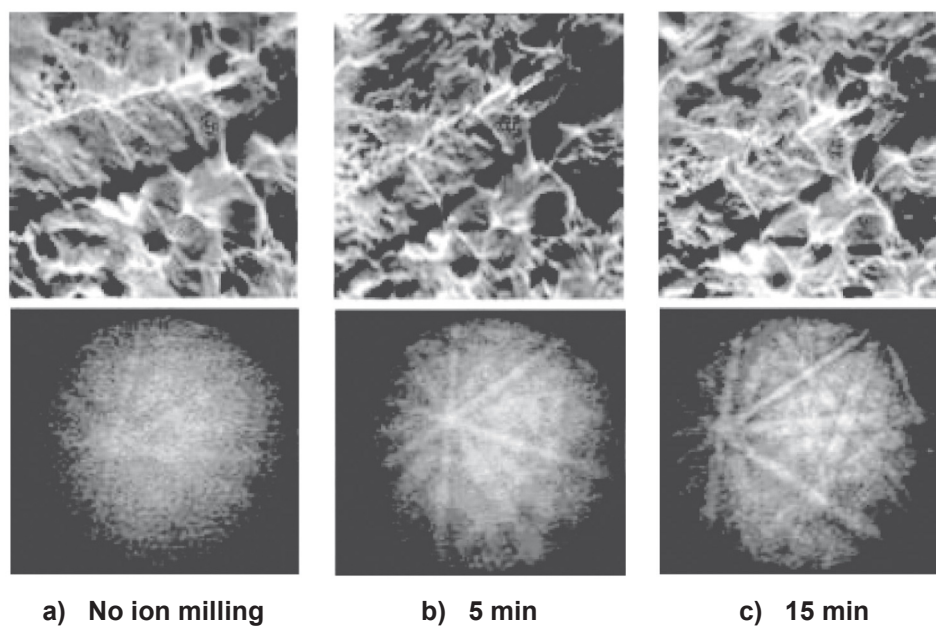
**Figure B.4 — Effect of different ion-milling times on quality
of pattern acquired with a copper specimen**

B.7.2   A focussed-ion beam (FIB) instrument is similar to the SEM, with the exception that a beam of excited ions is used instead of the conventional electron beam. The ion beam can be used to vaporize material from the specimen surface and is capable of "micro-machining" trenches and troughs and removing layers to reveal sections or surfaces of interest for imaging and EBSD examination. In the case of dual-beam instruments that have the capability of focussing both the ion and the electron beams onto the same region of the specimen, the prospect of specimen preparation *in situ* and under vacuum becomes a reality. The FIB technique is of interest with materials that are reactive or oxidize easily, which makes preparation by conventional methods impossible. FIB also creates the possibility of preparing materials that are too soft for conventional preparation. Because the technique can expose surfaces that are directly suitable for EBSD, without any further preparation or conditioning, and on a microscopic scale, it is especially useful in the semiconductor industry where ever smaller device geometry rules out conventional preparation methods.

B.8 Conductive coating [22]

Observing non-conductive specimens in the SEM is difficult due to charging effects. For EBSD work, charging effects include pattern degradation and beam drifting. The application of a thin, amorphous, conductive coating can eliminate charging effects. For such work, carbon is used as the primary coating material. While it is possible to use other materials (e.g. gold, gold-palladium or tungsten), carbon is best due to its low atomic number. Materials can be either sputtered or evaporated onto a specimen. As the coating thickness increases, the signal-to-noise ratio of the patterns decreases. A carbon coating of between 2 nm and 20 nm is recommended. This thickness provides adequate conductivity while still keeping the signal-to-noise ratio high. If this ratio drops to the point that the patterns are difficult to index, it is often useful to increase the acceleration voltage on the SEM, which increases beam penetration through the coating. If high atomic number materials (e.g. gold, gold-palladium or tungsten) are used for coating, the coating needs to be kept extremely thin (around 1 nm in thickness). Coating non-conductive specimens is often not necessary if a controlled-pressure SEM is used. Reducing the size of non-conducting specimens (e.g. to as small as 2 mm × 2 mm) can also help to reduce charging effects.

Annex C
(informative)

Brief introduction to crystallography and EBSP indexing, and other information useful for EBSD

C.1 General

This annex gives a very brief introduction to the concepts of crystallography as well as useful information for EBSD analysis. Since most users are likely to start with simple cubic phases, a section on how to index a cubic EBSP is also provided. This is useful for checking automatic EBSP analysis. It is recommended that standard introductory textbooks on crystallography also be consulted, e.g. References [7], [8] and [9].

C.2 Symmetry

An object has symmetry if it looks the same when rotated, translated or mirrored in a certain way. For example, a cube looks identical if it is rotated by 120° about its main diagonal. This 3-fold rotation axis is usually referred to as a "triad" axis. Figure C.1 shows a cube and an aluminium spherical Kikuchi map with their major symmetry elements labelled. EBSPs usually show a lot of symmetry, but the symmetry can be difficult to see if the EBSP is shown as a flat image. A spherical Kikuchi map is generally clearer.

Key

1   tetrad
2   triad
3   diad
4   mirror
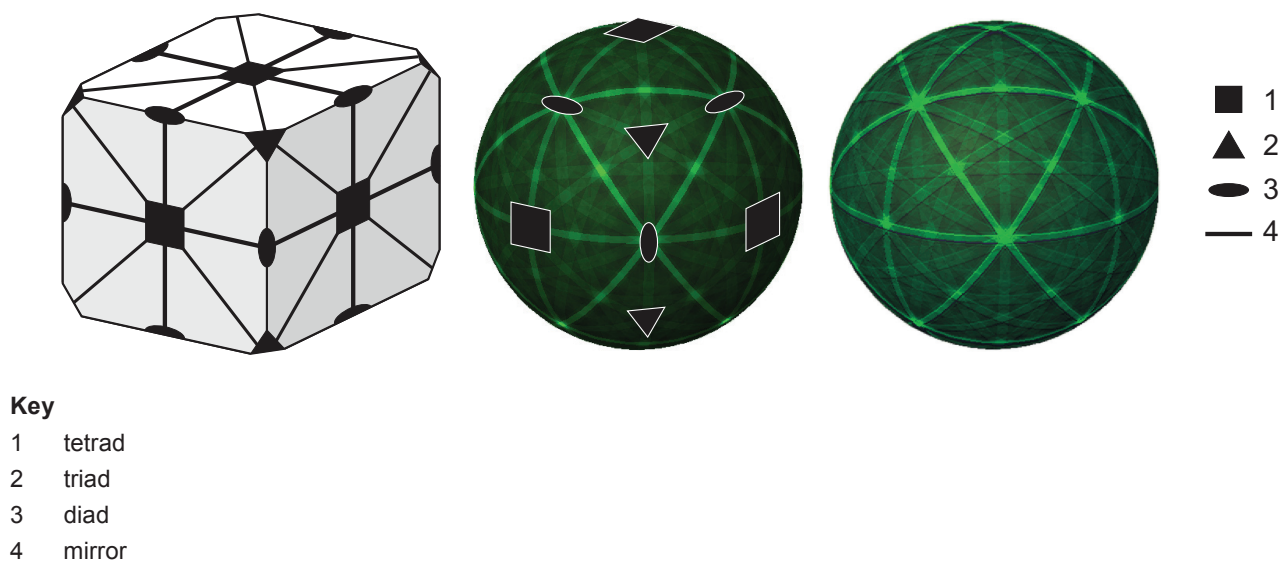
Figure C.1 — Schematic diagram showing the symmetries of a cube (left) and the symmetries of fcc EBSPs (centre), also shown as a spherical Kikuchi map (right)

A 2-fold rotation axis is usually called a diad, a 3-fold a triad, a 4-fold a tetrad and a 6-fold a hexad. A mirror means that everything on the left of the mirror must be mirrored on the right.

An example comprising a cube with EBSPs stuck on its faces and a spherical Kikuchi map for bcc iron is shown in Figure C.2. The spherical Kikuchi map will look the same if spun about one of the symbols, e.g. the triangular triad, or mirrored about one of the mirror planes. The cube with the EBSPs on it has the same symmetry.
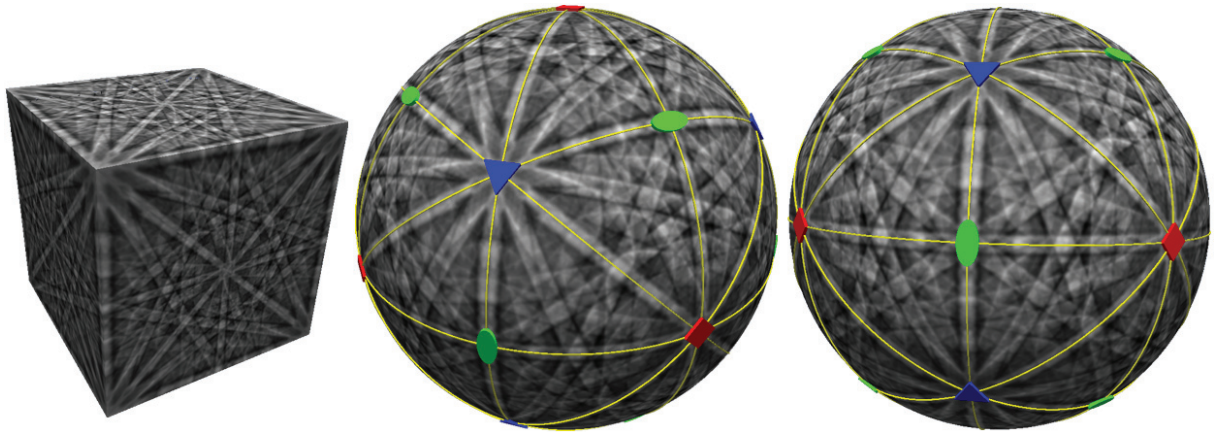
Figure C.2 — Six fcc EBSPs stuck on the surface of a cube (left) to show the symmetry of experimental EBSPs. The cube has been "inflated" to produce a spherical Kikuchi map (centre and right) and the symmetries are shown — mirrors as raised lines, diads as ellipses, triads as triangles and tetrads as squares.

C.3 The unit cell

A crystal consists of a group of atoms, called the basis, that are positioned relative to the crystal's unit cell and are repeated (almost) infinitely. The unit cell is described in terms of six parameters — three lengths, a, b, c, and three angles, α, β, γ (see Figure C.3). Lengths are usually given in nanometres or ångströms, angles in degrees. The coordinates of the atoms are given as fractions of the unit cell a-, b- and c-axes, with (0,0,0) being the origin, (½,½,½) the centre of the unit cell and (1,0,0) the a-axis.

a) Cell parameters	b) Atom positions	c) Crystal directions
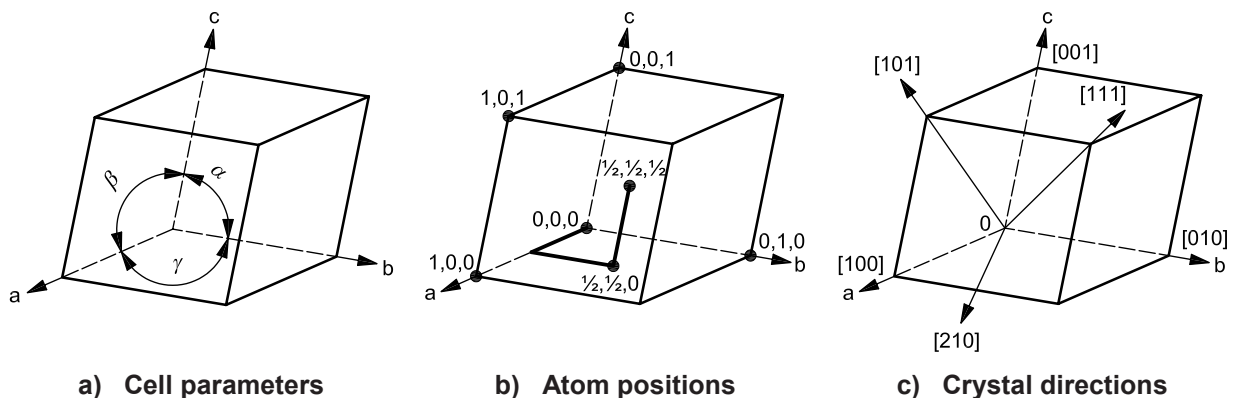
Figure C.3 — Schematic diagrams showing (left) the unit cell parameters, (centre) the fractional coordinates used to indicate the position of an atom within the unit cell and (right) the crystal directions or zones

C.4 Crystal directions

A crystal direction is usually written [$u\,v\,w$] and represents a vector direction from the origin of the crystal in multiples of the crystal axes a, b, c.

A family of symmetrically equivalent directions is written <$u\,v\,w$>. For example, in a cubic crystal, <1 1 1> is shorthand for [1 1 1], [–1 1 1], [1 –1 1], [1 1 –1], [1 –1 –1], [–1 1 –1], [–1 –1 1], [–1 –1 –1].

NOTE   Negative indices are often written with a bar above the number, e.g. [$\bar{1}1\bar{1}$] is the same as [–1 1 –1].

C.5 Crystal planes

A crystal plane is usually written $(h\,k\,l)$ and intersects the a-, b- and c-axes at $1/h$, $1/k$ and $1/l$, where h, k, and l are integers and are usually referred to as indices.

Examples of $(0\,0\,1)$, $(1\,1\,1)$ and $(1\,2\,2)$ planes, together with repeated planes, are shown in Figure C.4. Usually, the higher the indices, the closer the planes are together.

a) **(0 0 1) plane**   b) **(1 1 1) plane and (below)**   c) **(2 1 1) plane and repeat**
                        another, repeat, plane   **planes**
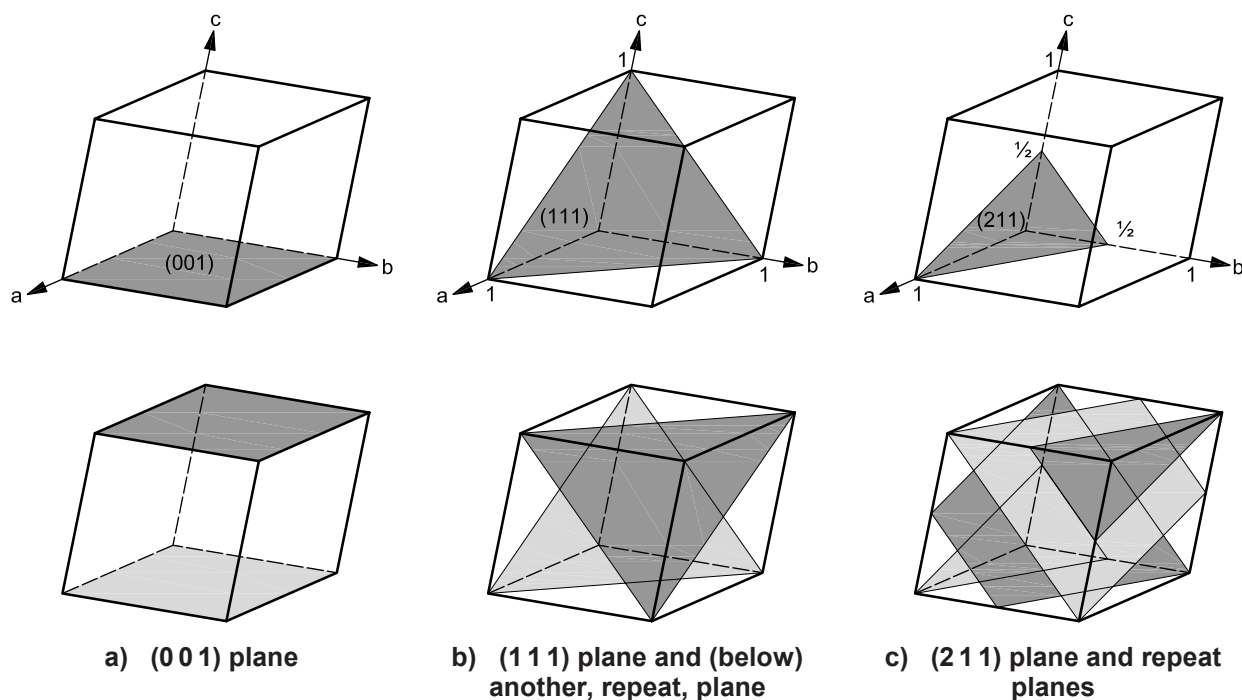
Figure C.4 — Schematic diagram showing examples of crystal planes

In EBSD, it is usually difficult to tell $(h\,k\,l)$ and $(-h\,-k\,-l)$ apart as they correspond to both edges of a Kikuchi band, so the convention is that $(h\,k\,l)$ usually refers to both the $(h\,k\,l)$ and the $(-h\,-k\,-l)$ planes. A family of symmetry-related planes is written $\{h\,k\,l\}$. For example, the cubic $\{2\,0\,0\}$ planes include $(2\,0\,0)$, $(0\,2\,0)$ and $(0\,0\,2)$ and will also imply $(-2\,0\,0)$, $(0\,-2\,0)$ and $(0\,0\,-2)$.

C.6 Crystal systems

Each crystal belongs to a crystal system which describes its basic symmetry. The usual crystal systems are given in Table C.1.

Table C.1 — Usual crystal systems

Crystal system	Unit cell parameters	Examples
Cubic	$a = b = c$, $\alpha = \beta = \gamma = 90°$	Iron, nickel, rock salt
Hexagonal	$a = b \neq c$, $\alpha = \beta = 90°$, $\gamma = 120°$	Titanium, apatite
Trigonal (rhombohedral [a])	$a = b \neq c$, $\alpha = \beta = 90°$, $\gamma = 120°$ ($a = b = c$, $\alpha = \beta = \gamma \neq 90°$ and $<120°$)	Quartz, calcite, haematite
Tetragonal	$a = b \neq c$, $\alpha = \beta = \gamma = 90°$	Tin, zircon
Orthorhombic	$a \neq b \neq c$, $\alpha = \beta = \gamma = 90°$	$YBa_2Cu_3O_7$, sulfur, $PbSO_4$
Monoclinic [b]	$a = c \neq b$, $\alpha = \gamma = 90° \neq \beta$ which is $>90°$	Clinopyroxene
Triclinic (anorthic)	$a \neq b \neq c$, $\alpha \neq \beta \neq \gamma \neq 90°$	Kyanite, copper sulfate
NOTE Some modern textbooks merge trigonal and rhombohedral with hexagonal.		

[a] Some trigonal crystals can also be represented using a rhombohedral unit cell, which is basically a cube that has been squashed or stretched along a diagonal. Three rhombohedral unit cells will fit into the hexagonal unit cell, as shown in Figure C.5. There are also two possible unit cells for rhombohedral, the "obverse" and the "reverse", which are mirror images of each other.

[b] By convention, monoclinic crystals have the b-axis unique, and this axis is shown vertically. This is not always the case, and older crystal data may have the a- or c-axis unique; this is referred to as an alternative setting. The orthorhombic crystal system also has a wide range of alternative settings in which the order of the a-, b- and c-axes are effectively permutated.

C.7 Laue groups

The Laue groups (see Table C.2) describe the essential symmetry of the EBSPs, i.e. the diffraction symmetry after Friedel's law has been applied. Friedel's law means that we cannot easily tell $(h\,k\,l)$ and $(\bar{h}\,\bar{k}\,\bar{l})$ apart because the lattice looks very similar to an electron travelling backwards or forwards.

Table C.2 — Laue groups

Laue group	Examples
High cubic	Aluminium, nickel, galena
Low cubic	Pyrite (FeS_2)
High hexagonal	Titanium
Low hexagonal	Apatite
High trigonal	Quartz, calcite
Low trigonal	Dolomite
High tetragonal	Chalcopyrite
Low tetragonal	Wulfenite
Orthorhombic	$YBa_2Cu_3O_7$, magnesium sulfate
Monoclinic	Zirconia
Triclinic	Copper sulfate, anorthite, albite
NOTE For some geological phases, the "low" groups are quite important and can have unexpected symmetries, for example pyrite (FeS_2), which is low cubic, has no 4-fold axes.	

C.8 Bravais lattices

The Bravais lattice description allows the basis (the group of atoms to be duplicated) to be copied and placed at special sites in the unit cell. This is known as centring. The special sites are shown in Figure C.5 as black spheres. In some cases they will correspond to single atoms, but, in general, this is not necessary.

An undecorated unit cell has the symbol P (primitive), while one with a special site at the centre of the unit cell has the symbol I (internal). The centres of the faces can also have sites. If all the faces are centred, then it is referred to as F (face); if only one pair of faces is centred, then it will usually be the C face, although A and B centring can also occur.

Cubic P   **Cubic I**   **Cubic F**

Hexagonal P   **Trigonal R**   **Tetragonal P**   **Tetragonal I**

Orthorhombic P   **Orthorhombic C**   **Orthorhombic I**   **Orthorhombic F**

Monoclinic P   **Monoclinic C**   **Triclinic P**
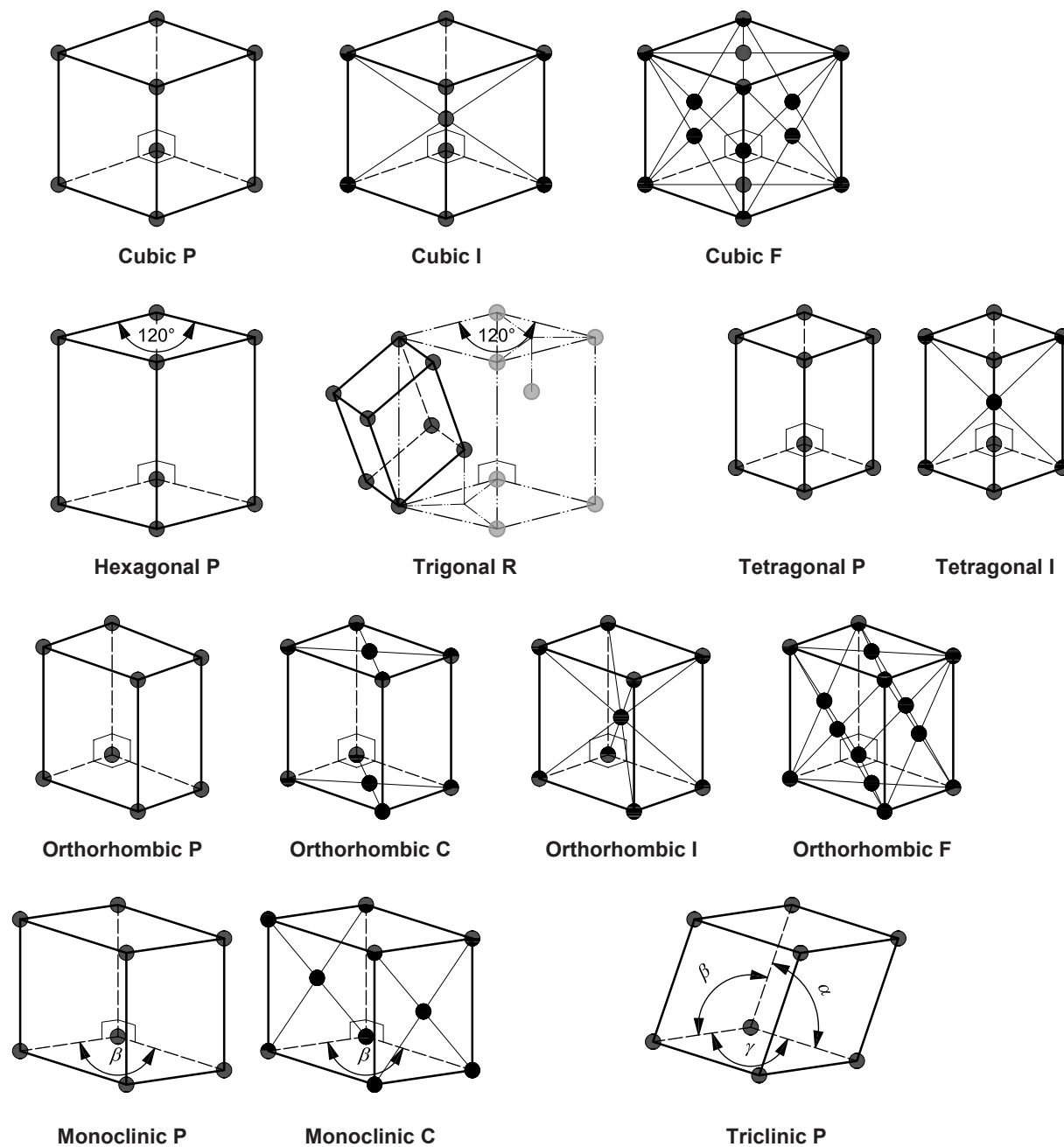
NOTE   For the trigonal (rhombohedral) cell, the alternative hexagonal triple unit cell is also shown (see second row). For monoclinic, the unique b-axis option is indicated by the angle β.

Figure C.5 — Schematic diagram showing the Bravais lattices
(The crystal system and centring are indicated)

C.9 Manual indexing of a cubic EBSP

It is relatively easy to index a cubic EBSP manually and it is a useful skill when checking automatic indexing of EBSPs. Most EBSD systems have a means to simulate an EBSP at a chosen orientation. It is easier to learn from a spherical Kikuchi map, as an EBSP may be viewed from any orientation with minimum projection distortion (most EBSPs are gnomonic projections).

The first thing to look for is symmetry — try to identify mirrors, 2-fold axes (diads) or, even better, a 3-fold (triad) or 4-fold (tetrad) axis. Once these are identified, use the map to locate other symmetry elements. However, the gnomonic projection of the EBSP can sometimes make the symmetry difficult to see, especially when zones are near the edges of the EBSP.

The small parts of EBSPs shown in Figure C.6 illustrate mirrors, diads, triads and tetrads for face- and body-centred cubics. Further explanation is given in Table C.3.

| a) **Iron bcc mirror** | b) **Iron bcc 3-fold (triad)** | c) **Iron bcc 4-fold (tetrad)** | d) **Iron bcc 2-fold (diad)** |

| e) **Iron fcc mirror** | f) **Iron fcc 3-fold (triad)** | g) **Iron fcc 4-fold (tetrad)** | h) **Iron fcc 2-fold (diad)** |
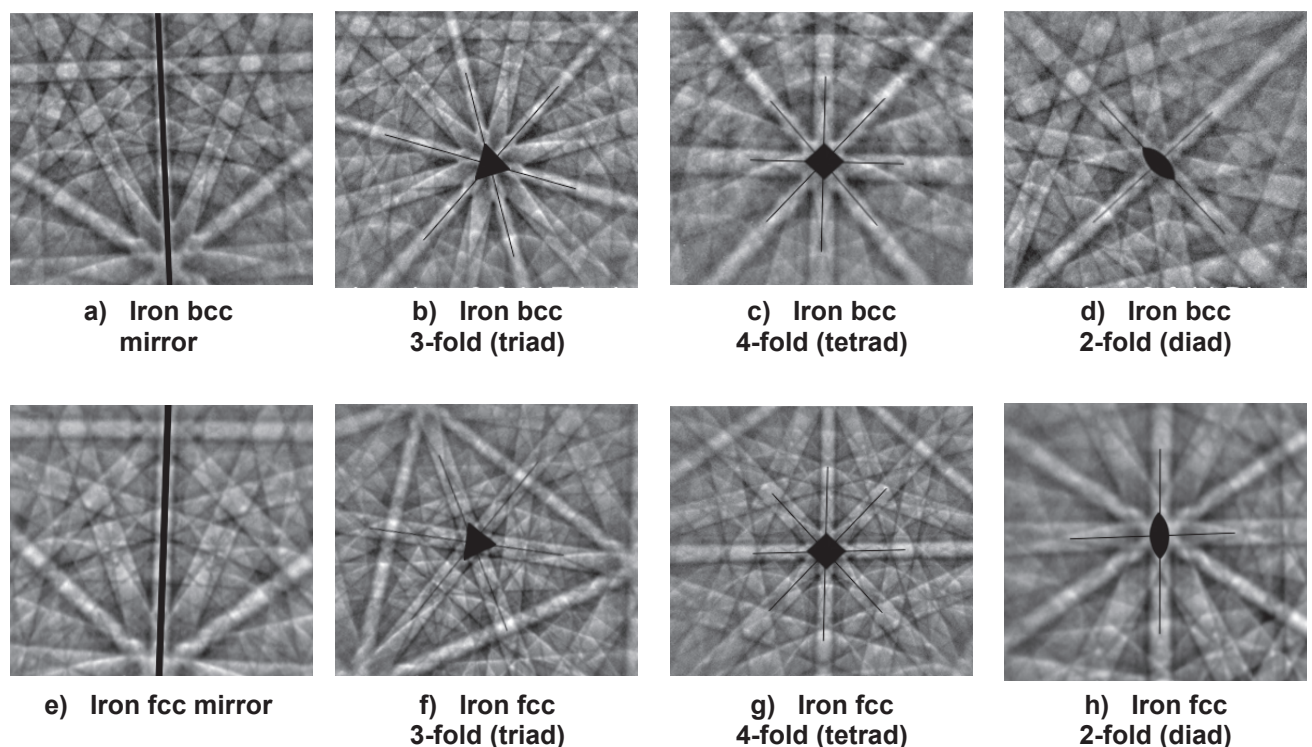
Figure C.6 — Examples of parts of iron bcc (top row) and fcc (bottom row) EBSPs, showing mirrors, triads (3-fold rotations), tetrads (4-fold) and diads (2-fold), as indicated

Table C.3 — Symmetry for fcc and bcc

Zone	Symmetry for fcc and bcc	Comments
<0 0 1>	4-fold with four mirror planes running through	Can sometimes be mistaken for <1 1 0> in fcc.
<1 1 1>	3-fold with three mirror planes running through	For bcc, it looks like a 6-pointed snowflake; for fcc, there is a triangle around it.
<1 1 0>	2-fold with two mirrors running through	
<1 1 2>	On a mirror running from <0 0 1> to <1 1 1>	Roughly half-way between a 4-fold <0 0 1> and a 3-fold <1 1 1>. For fcc, it looks like the centre of a bow tie.
<1 1 4>	On a mirror running from <0 0 1> to <1 1 1>	Very close to <0 0 1> and, for fcc, it can easily be mistaken for <1 1 1> with a triangle around it.

C.10   Examples of indexed cubic EBSPs

Figure C.7 gives examples of EBSPs in which the symmetries have been highlighted and the main zones marked. They can be used as self-test exercises by covering up the centre and right-hand images and locating the mirrors, diads, triads and tetrads and then identifying the main zones.

NOTE   It is not critical that the reader be able recognize the indices shown (for example [0 0 1] is equivalent to [1 0 0]).
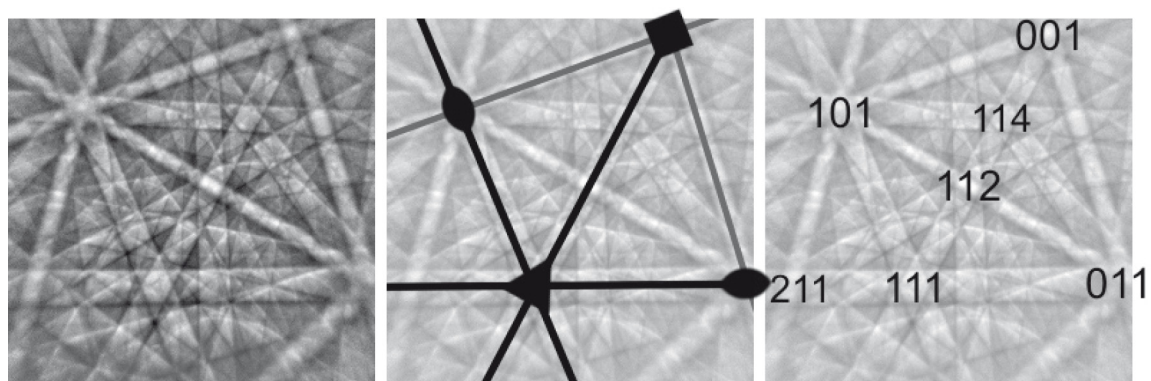
Example 1
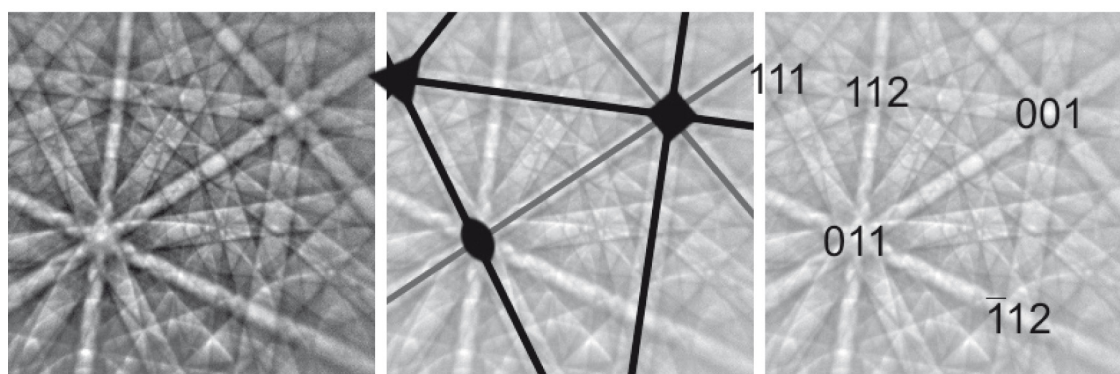
Example 2
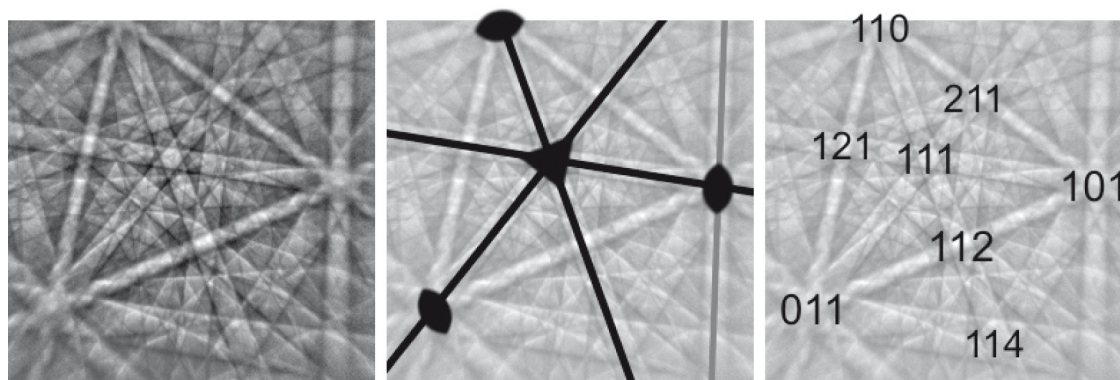
Example 3

Figure C.7 — Nickel fcc EBSP (left) and the main symmetries (centre) and indexed zones (right)
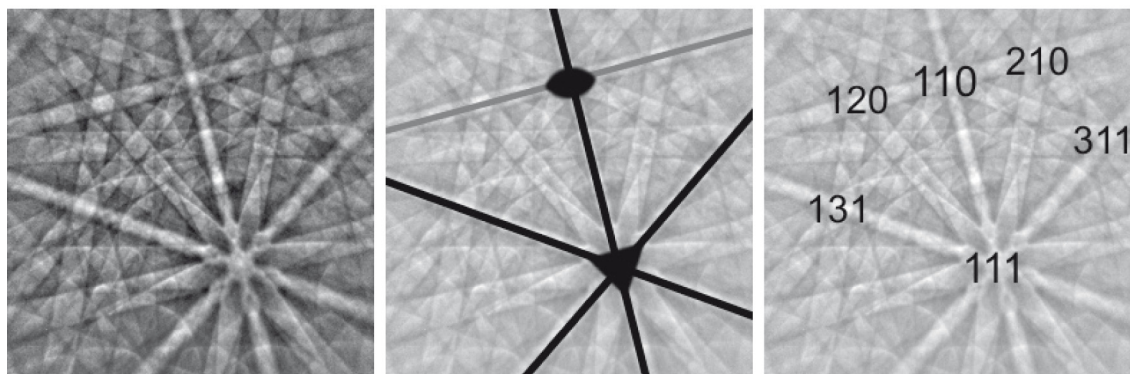
Example 1
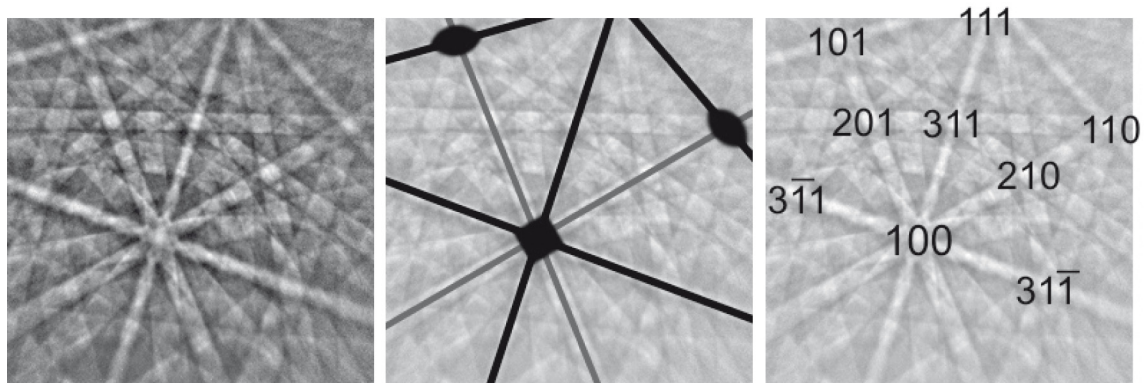
Example 2

Figure C.8 — Iron bcc EBSP (left) and the main symmetries (centre) and indexed zones (right)

C.11   Hexagonal indices

When working with hexagonal and trigonal phases, four-digit indices are frequently used for planes ($h\,k\,i\,l$) and for crystal directions [$u\,v\,t\,w$] as they show equivalent planes and directions more readily. The fourth digit comes from having three symmetrically arranged axes, as shown in Figure C.9.

a)   Three-digit indices: ($h\,k\,l$) and [$u\,v\,w$]

b)   Four-digit indices: ($h\,k\,i\,l$) and [$u\,v\,t\,w$]
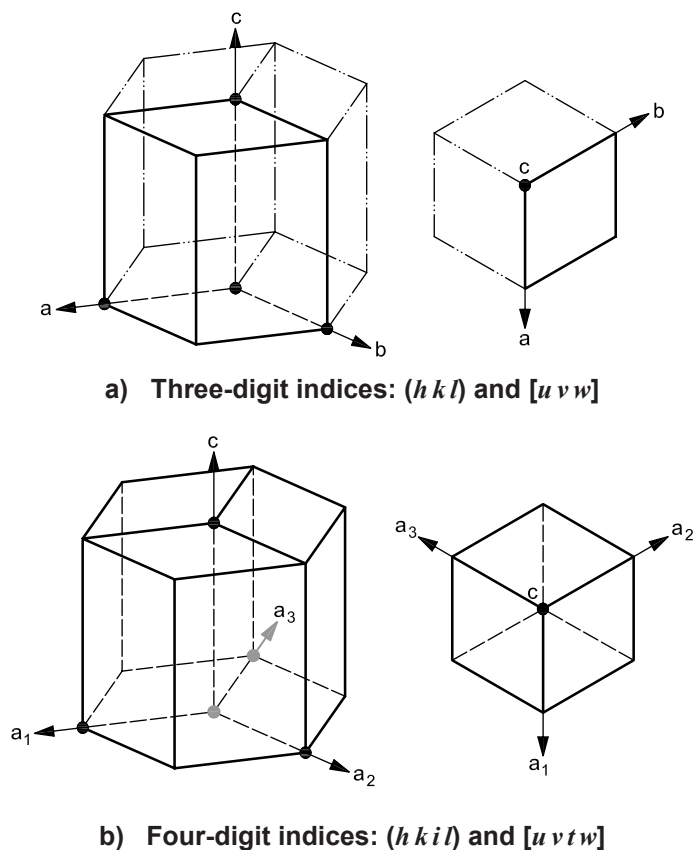
Figure C.9 — Schematic diagram showing hexagonal indices for crystal planes (left in each case) and directions (right in each case)

Planes are easy to convert from three-digit indices to four-digit indices. The third digit is simply minus the sum of the first two:

$$(h\,k\,i\,l) = (h_3, k_3, -(h_3 + k_3), l_3)$$

where ($h_3\,k_3\,l_3$) is the three-digit plane.

Frequently, the third digit will be shown as a dot, e.g. ($1\,2\,.\,4$) or ($0\,1\,.\,2$).

To convert from four-digit planes to three, drop the third index, i:

($h\,k\,l$)	($h\,k\,i\,l$)	($h\,k\,l$)	($h\,k\,i\,l$)	($h\,k\,l$)	($h\,k\,i\,l$)
($1\,0\,0$)	($1\,0\,{-}1\,0$)	($2\,1\,0$)	($2\,1\,{-}3\,0$)	($1\,0\,1$)	($1\,0\,{-}1\,1$)
($1\,1\,0$)	($1\,1\,{-}2\,0$)	($2\,1\,1$)	($2\,1\,{-}3\,1$)	($1\,1\,1$)	($1\,1\,{-}2\,1$)
($0\,0\,1$)	($0\,0\,0\,1$)	($0\,1\,0$)	($0\,1\,{-}1\,0$)	($1\,2\,0$)	($1\,2\,{-}3\,0$)
($0\,1\,1$)	($0\,1\,{-}1\,1$)	($-1\,1\,0$)	($-1\,1\,0\,0$)	($1\,1\,2$)	($1\,1\,{-}2\,2$)

The following formulae, sometimes known as Miller and Miller-Bravais formulae, respectively, convert to and from three-digit crystal direction indices, $[u_3\, v_3\, w_3]$, and four-digit crystal direction indices, $[u_4\, v_4\, t\, w_4]$:

$$\left[u_4 = \frac{1}{3}(2u_3 - v_3), \quad v_4 = \frac{1}{3}(2v_3 - u_3), \quad t = -\frac{1}{3}(u_3 + v_3), \quad w_4 = w_3 \right]$$

$$\left[u_3 = u_4 - t, \quad v_3 = v_4 - t, \quad w_3 = w_4 \right]$$

[u v w]	[u v t w]
[1 0 0]	[2 −1 −1 0]
[1 1 0]	[1 1 −2 0]
[0 0 1]	[0 0 0 1]
[0 1 1]	[−1 2 −1 3]

[u v w]	[u v t w]
[2 1 0]	[1 0 −1 0]
[2 1 1]	[1 0 −1 1]
[0 1 0]	[−1 2 −1 0]
[−1 1 0]	[−1 1 0 0]

[u v w]	[u v t w]
[1 0 1]	[2 −1 −1 3]
[1 1 1]	[1 1 −2 3]
[1 2 0]	[0 1 −1 0]
[1 1 2]	[1 1 −2 6]

C.12 Useful formulae and information

C.12.1 Symbols

The following symbols are used in this clause:

a, b, c, α, β, γ	the unit cell parameters
Ω	the unit cell volume
λ	the electron wavelength at the relevant accelerating voltage
kV	the accelerating voltage of the electron beam, usually 20 kV
d_{hkl}	the lattice spacing for planes $(h\, k\, l)$
θ_{Bragg}	the Bragg diffraction angle (the width of a Kikuchi band is $2\theta_{Bragg}$)
n	an integer
$(h\, k\, l)$	a plane
$[u\, v\, w]$	a crystal direction
$(h\, k\, i\, l)$	a plane, using four-digit, hexagonal, notation
$[u\, v\, t\, w]$	a crystal direction, using four-digit, hexagonal, notation
θ	the angle between a pair of planes or a pair of zones

C.12.2 Electron wavelength as a function of accelerating voltage

$$\lambda \approx \frac{0{,}038\ 78}{\sqrt{kV}}\ nm \quad \text{(non-relativistic)}$$

Accelerating voltage kV	Wavelength nm
5	0,017 3
10	0,012 3
15	0,010 0
20	0,008 7
30	0,007 1

C.12.3 Interplanar spacing for plane ($h\,k\,l$)

Bragg diffraction equation:

$$\lambda = 2d_{hkl}\sin\theta_{Bragg} \quad \text{or} \quad \theta_{Bragg} = \sin^{-1}\left(\frac{\lambda}{2d_{hkl}}\right)$$

Cubic

$$d_{hkl} = \frac{a}{\sqrt{\left(h^2 + k^2 + l^2\right)}}\ nm$$

Hexagonal

$$d_{hkl} = \frac{1}{\sqrt{\frac{4}{3a^2}\left(h^2 + k^2 + hk\right) + \frac{l^2}{c^2}}}\ nm$$

Tetragonal and orthorhombic

$$d_{hkl} = \frac{1}{\sqrt{\frac{h^2}{a^2} + \frac{k^2}{b^2} + \frac{l^2}{c^2}}}\ nm$$

The formulae for other types of lattice are complex and can be found in standard books on crystallography, e.g. References [7], [8] and [9].

C.12.4 Unit cell volume

Cubic

$$\Omega = a^3$$

Hexagonal

$$\Omega = \frac{\sqrt{3}}{2}a^2c \quad (\approx 0{,}866a^2c)$$

Tetragonal and orthorhombic

$$\Omega = abc$$

C.12.5 Angle between two planes ($h_1\,k_1\,l_1$) and ($h_2\,k_2\,l_2$)

Cubic

$$\theta = \cos^{-1}\left(\frac{h_1h_2 + k_1k_2 + l_1l_2}{\sqrt{\left(h_1^2 + k_1^2 + l_1^2\right)\left(h_2^2 + k_2^2 + l_2^2\right)}}\right)$$

Hexagonal

$$\theta = \cos^{-1}\left(\frac{h_1h_2 + k_1k_2 + \frac{1}{2}\left(h_1k_2 + h_2k_1\right) + \frac{3a^2}{4c^2}l_1l_2}{\sqrt{\left(h_1^2 + k_1^2 + h_1k_1 + \frac{3a^2}{4c^2}l_1^2\right)\left(h_2^2 + k_2^2 + h_2k_2 + \frac{3a^2}{4c^2}l_2^2\right)}}\right)$$

Tetragonal and orthorhombic

$$\theta = \cos^{-1}\left(\frac{\frac{h_1h_2}{a^2} + \frac{k_1k_2}{b^2} + \frac{l_1l_2}{c^2}}{\sqrt{\left(\frac{h_1^2}{a^2} + \frac{k_1^2}{b^2} + \frac{l_1^2}{c^2}\right)\left(\frac{h_2^2}{a^2} + \frac{k_2^2}{b^2} + \frac{l_2^2}{c^2}\right)}}\right)$$

C.12.6 To find the zone [$u\,v\,w$] that is perpendicular to plane ($h\,k\,l$)

Cubic

$$\frac{u}{h} = \frac{v}{k} = \frac{w}{l} \qquad\qquad \frac{h}{u} = \frac{k}{v} = \frac{l}{w}$$

Hexagonal

$$\frac{u}{2h+k} = \frac{v}{2k+h} = \frac{2w}{3l}\frac{c^2}{a^2} \qquad\qquad \frac{h}{2u-v} = \frac{k}{2v-u} = \frac{l}{2w}\frac{a^2}{c^2}$$

Tetragonal and orthorhombic

$$\frac{ua^2}{h} = \frac{vb^2}{k} = \frac{wc^2}{l} \qquad\qquad \frac{h}{ua^2} = \frac{k}{vb^2} = \frac{l}{wc^2}$$

C.12.7 Relationships between zones and planes

For a plane ($h\,k\,l$) that passes through a zone [$u\,v\,w$]:

$$hu + kv + lw = 0$$

For a plane ($h\,k\,l$) which intersects the zones [$u_1\,v_1\,w_1$] and [$u_2\,v_2\,w_2$]:

$$h = (u_1w_2 - u_2w_1) \qquad k = (w_1u_2 - w_2u_1) \qquad l = (u_1v_2 - u_2v_1)$$

For a zone [$u\,v\,w$] which lies at the intersection of the planes ($h_1\,k_1\,l_1$) and ($h_2\,k_2\,l_2$):

$$u = (k_1l_2 - k_2l_1) \qquad v = (l_1h_2 - l_2h_1) \qquad w = (h_1k_2 - h_2k_1)$$

C.12.8 Conditions for a Kikuchi band to be visible

The intensity of a Kikuchi band can be estimated using the kinematical diffraction model [2],[4]. In some cases, the calculated structure will be predicted to be zero due to scattering from one atom being cancelled out by that from a neighbouring atom. For these cases, it is possible to produce rules that predict which reflectors, or Kikuchi bands, will be visible and which should have a zero structure factor and low intensity (see Table C.4).

Table C.4 — Rules governing visibility of Kikuchi bands

Lattice type		Conditions for Kikuchi band to be visible	Example planes
Body-centred	I	$h + k + l = 2n$	{1 1 0} {2 0 0} {1 1 2} {2 2 0} {0 1 3} {2 2 2} {1 2 3} {4 0 0}
Face-centred	F	h, k and l all odd or all even	{1 1 1} {2 0 0} {2 2 0} {1 1 3} {2 2 2} {4 0 0} {1 3 3} {2 4 0}
Diamond type		$h + k + l$ is odd or $h + k + l = 4n$	{1 1 1} {2 2 0} {4 0 0} {1 1 3} {2 2 4} {1 3 3} {4 4 0} {2 6 0}
Hexagonal close-packed		$h + 2k \neq 3n$ or l is even	{0 0 2} {0 1 1} {1 1 0} {1 0 0} {1 1 2} {0 0 4} {0 1 3} {2 0 1} or {0 0 0 2} {0 1 −1 1} {1 1 2 0} {1 0 −0 0} {1 1 −2 2} {0 0 0 4}
A-centred	A	$k + l = 2n$	
B-centred	B	$h + l = 2n$	
C-centred	C	$h + k = 2n$	

Since most EBSD software uses the kinematical diffraction model to predict the expected reflectors, it should always be borne in mind that these reflectors could be wrong, especially with more complex structures. The ability to edit or add/remove reflectors is a useful tool, but should be used with care.

NOTE 1   The diamond lattice consists of two interpenetrating fcc Bravais lattices which are displaced along the body diagonal of the cubic cell by one-quarter the length of the diagonal. It is not a Bravais lattice.

NOTE 2   These rules only hold for simple structures and if double diffraction effects are weak. For example, with silicon, the kinematical model predicts that the {2 0 0} and {2 2 2} planes should not be visible. As expected, the {2 0 0} planes do not appear in a silicon EBSP. However, {2 2 2} is present, but weak due to double diffraction, as shown in Figure C.10.
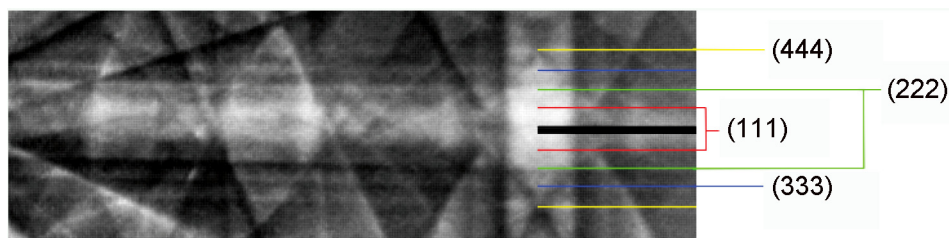

Figure C.10 — Detail of a silicon EBSP showing the (1 1 1) planes
[the (2 2 2) plane is forbidden and should not be visible]

C.12.9 Cubic interzonal and interplanar angles

Table C.5 lists the commonest angles, in degrees, between two zones or two planes in the families indicated.

Table C.5 — Commonest angles between two planes or two zones

Families		Inter-zonal or inter-planar angles degrees					
1 0 0	1 0 0	90,00					
	1 1 0	45,00	90,00				
	1 1 1	54,74					
	2 1 0	26,57	63,43	90,00			
	2 1 1	35,26	65,91				
	2 2 1	48,19	70,53				
1 1 0	1 1 0	60,00	90,00				
	1 1 1	35,26	90,00				
	2 1 0	18,43	50,77	71,57			
	2 1 1	30,00	54,74	73,22	90,00		
	2 2 1	19,47	45,00	76,37	90,00		
1 1 1	1 1 1	70,53	109,47				
	2 1 0	39,23	75,04				
	2 1 1	19,47	61,87	90,00			
	2 2 1	15,79	54,74	78,90			
2 1 0	2 1 0	36,87	53,13	66,42	78,46	90,00	
	2 1 1	24,09	43,09	56,79	79,48	90,00	
	2 2 1	26,57	41,81	53,40	63,43	72,65	90,00
2 1 1	2 1 1	33,56	48,19	60,00	70,53	80,41	
	2 2 1	17,72	35,26	47,12	65,91	74,21	82,18
0 0 1	1 1 4	19,47					

C.12.10 Crystallographic information for selected cubic phases

Phase	Laue	Space group	Unit cell	Atoms
Aluminium, fcc	m3m	225 Fm$\bar{3}$m	a = 4,050 Å	Al 4a (0,0,0) (0,½,½) (½,0,½) (½,½,0)
Nickel, fcc	m3m	225 Fm$\bar{3}$m	a = 3,524 Å	Ni 4a (0,0,0) (0,½,½) (½,0,½) (½,½,0)
Copper, fcc	m3m	225 Fm$\bar{3}$m	a = 3,614 Å	Cu 4a (0,0,0) (0,½,½) (½,0,½) (½,½,0)
Iron, fcc	m3m	225 Fm$\bar{3}$m	a = 3,660 Å	Fe 4a (0,0,0) (0,½,½) (½,0,½) (½,½,0)
Iron, bcc	m3m	229 Im$\bar{3}$m	a = 2,866 Å	Fe 2a (0,0,0) (½,½,½)
Silicon	m3m	227 Fd$\bar{3}$m	a = 5,431 Å	Si 8a (0,0,0) (0,½,½) (½,0,½) (½,½,0) (¼,¼,¼) (¼,¾,¾) (¾,¼,¾) (¾,¾,¼)
Diamond	m3m	227 Fd$\bar{3}$m	a = 3,567 Å	C 8a (0,0,0) (0,½,½) (½,0,½) (½,½,0) (¼,¼,¼) (¼,¾,¾) (¾,¼,¾) (¾,¾,¼)
GaAs	m3m	216 F$\bar{4}$3m	a = 5,652 Å	As 4a (0,0,0) (0,½,½) (½,0,½) (½,½,0); Ga 4c (¼,¼,¼) (¼,¾,¾) (¾,¼,¾) (¾,¾,¼)
Sphaelerite, ZnS	m3m	216 F$\bar{4}$3m	a = 5,400 Å	S 4a (0,0,0) (0,½,½) (½,0,½) (½,½,0); Zn 4c (¼,¼,¼) (¼,¾,¾) (¾,¼,¾) (¾,¾,¼)
Galena, PbS	m3m	225 Fm$\bar{3}$m	a = 5,936 Å	Pb 4a (0,0,0) (0,½,½) (½,0,½) (½,½,0); S 4b (½,½,½) (½,0,0) (0,½,0) (0,0,½)
Halite, NaCl	m3m	225 Fm$\bar{3}$m	a = 5,640 Å	Cl 4a (0,0,0) (0,½,½) (½,0,½) (½,½,0); Na 4b (½,½,½) (½,0,0) (0,½,0) (0,0,½)
Pyrite, FeS$_2$	m3	205 Pa$\bar{3}$	a = 5,418 Å	Fe 4a (0,0,0) (0,½,½) (½,0,½) (½,½,0); S 8c (0,387, 0,387, 0,387) (0,113, 0,613, 0,887) (0,613, 0,887, 0,113) (0,887, 0,113, 0,613) (0,613, 0,613, 0,613) (0,887, 0,387, 0,113) (0,387, 0,113, 0,887) (0,113, 0,887, 0,387)
Titanium, cubic	m3m	229 Im$\bar{3}$m	a = 3,31 Å	Ti 2a (0,0,0) (½,½,½)

C.12.11 Crystallographic information for selected hexagonal, tetragonal and orthorhombic phases

Phase	Laue	Space group	Unit cell	Atoms
Titanium, hcp	6/mmm	194 P6$_3$/mmc	a = 2,950 Å c = 4,681 Å	Ti 2c (⅓,⅔,¼) (⅔,⅓,¾)
Magnesium	6/mmm	194 P6$_3$/mmc	a = 3,209 Å c = 5,210 Å	Mg 2c (⅓,⅔,¼) (⅔,⅓,¾)
Zinc	6/mmm	194 P6$_3$/mmc	a = 2,665 Å c = 4,947 Å	Zn 2c (⅓,⅔,¼) (⅔,⅓,¾)
BaTiO$_3$, tetragonal	4/mmm	99 P4mm	a = 3,995 Å c = 4,034 Å	Ba 1a (0,0,0); O 2c (½, 0, 0,486) (0, ½, 0,486); Ti 1b (½, ½, 0,512); O 1b (½, ½, 0,023)
Tin	4/mmm	141 I4$_1$/amd	a = 5,832 Å c = 3,181 Å	Sn 4a (0,0,0) (½,½,½) (0,½,¼) (½,0,¾)
YBa$_2$Cu$_3$O$_7$	mmm	47 Pmmm	a = 3,818 Å b = 3,886 Å c = 11,70 Å	Y 1h (½,½,½); Ba 2t (½, ½, 0,186) (½, ½, 0,814); Cu 1a (0,0,0) Cu 2q (0, 0, 0,356) (0, 0, 0,644); O 1e (0,½,0); O 2q (0, 0, 0,158) (0, 0, 0,842); O 2r (0, ½, 0,378) (0, ½, 0,622); O 2s (½, 0, 0,379) (½, 0, 0,621)

C.12.12 Cubic coincidence site lattice (CSL) misorientation relationships

See Reference [10] for details.

Σ	Axis	Angle degrees	Brandon angle degrees	Σ	Axis	Angle degrees	Brandon angle degrees
3	[1 1 1]	60,000	8,66	33b	[3 1 1]	33,557	2,61
5	[1 0 0]	36,870	6,71	33c	[1 1 0]	58,992	2,61
7	[1 1 1]	38,213	5,67	35a	[2 1 1]	34,040	2,54
9	[1 1 0]	38,942	5,00	35b	[3 3 1]	43,230	2,54
11	[1 1 0]	50,479	4,52	37a	[1 0 0]	18,920	2,47
13a	[1 0 0]	22,620	4,16	37b	[3 1 0]	43,130	2,47
13b	[1 1 1]	27,796	4,16	37c	[1 1 1]	50,570	2,47
15	[2 1 0]	48,190	3,87	39a	[1 1 1]	32,210	2,40
17a	[1 0 0]	28,073	3,64	39b	[3 2 1]	50,130	2,40
17b	[2 2 1]	61,928	3,64	41a	[1 0 0]	12,680	2,34
19a	[1 1 0]	26,525	3,44	41b	[2 1 0]	40,880	2,34
19b	[1 1 1]	46,826	3,44	41c	[1 1 0]	55,880	2,34
21a	[1 1 1]	21,787	3,27	43a	[1 1 1]	15,180	2,29
21b	[2 1 1]	44,415	3,27	43b	[2 1 0]	27,910	2,29
23	[3 1 1]	40,459	3,13	43c	[3 3 2]	60,770	2,29
25a	[1 0 0]	16,260	3,00	45a	[3 1 1]	28,620	2,24
25b	[3 3 1]	51,684	3,00	45b	[2 2 1]	36,870	2,24
27a	[1 1 0]	31,586	2,89	45c	[2 2 1]	53,130	2,24
27b	[2 1 0]	35,431	2,89	47a	[3 3 1]	37,070	2,19
29a	[1 0 0]	43,603	2,79	47b	[3 2 0]	43,660	2,19
29b	[2 2 1]	46,397	2,79	49a	[1 1 1]	43,580	2,14
31a	[1 1 1]	17,897	2,69	49b	[5 1 1]	43,580	2,14
31b	[2 1 1]	52,200	2,69	49c	[3 2 2]	49,220	2,14
33a	[1 1 0]	20,050	2,61				

Bibliography

[1] Chinese national standard GB/T 19501-2004, *General guide for electron backscatter diffraction analysis*

[2] RANDLE, V., *Electron Backscatter Diffraction*, Guide Book Series, Published by Oxford Instruments, Microanalysis Group, 1994

[3] KATRAKOVA, D., and MÜCKLICH, F., Specimen Preparation for Electron Backscatter Diffraction, *Prakt. Metallogr.*, Part 1: Metals, **38** (2001), 10, pp. 547-564; Part 2: Ceramics, **39** (2002), 12, pp. 644-662

[4] SCHWARTZ, A.J., *Electron Backscatter Diffraction in Materials Science*, Kluwer Academic/Plenum Publishers, 2000, ISBN 0-306-46487-X

[5] RANDLE, V., *Microtexture Determination and Its Applications*, Maney Publishing, 2003, ISBN 1902653831

[6] RANDLE, V., and ENGLER, O., *Texture Analysis, Macrotexture, Microtexture and Orientation Mapping*, Taylor and Francis, 2000, ISBN 9056992244

[7] MCKIE, D., and MCKIE, C., *Essentials of Crystallography*, Blackwell Scientific Publishers, 1986, ISBN 0-632-01574-8

[8] PHILIPS, F.C., *An Introduction to Crystallography*, fourth edition, Oliver and Boyd, 1971

[9] HAMMOND, C., *The Basics of Crystallography and Diffraction*, IUCr, 1997, ISBN 0-19-855945-3

[10] BRANDON, D.G., The Structure of High-Angle Grain Boundaries, *Acta Metall.*, **14** (1966), pp. 1479-1484

[11] HOUGH, P.V.C., *Method and Means for Recognizing Complex Patterns*, US patent 3,069,654

[12] LEAVERS, V.F., *Shape Detection in Computer Vision Using the Hough Transform*, Springer-Verlag, 1992, ISBN 3-540-19723-0

[13] PRIOR, D.J., BOYLE, A.P., BRENKER, F., CHEADLE, M.C., DAY, A.P., and LOPEZ, G., The application of electron backscatter diffraction and orientation contrast imaging in the SEM to textural problems in rocks, *American Mineralogist*, **84** (1999), pp. 1741-1759

[14] TIAN, Q., YIN, F., SAKAGUCHI, T., and NAGAI, K., Reverse transformation behavior of a prestrained MnCu alloy, *Acta Mater.*, **54** (2006), pp. 1805-1813

[15] DINGLEY, D., and FIELD, D.P., Electron backscatter diffraction and orientation imaging microscopy, *Mater. Sci. Tech.*, **13** (1997), pp. 69-78

[16] LE PAGE, Y., Ab-Initio Primitive Cell Parameters from Single Convergent-Beam Electron Diffraction Patterns: A Converse Route to the Identification of Microcrystals with Electrons, *Microscopy Research and Technique*, **21** (1992), pp. 158-165

[17] MICHAEL, J.R., *et al.*, *Crystal phase identification*, 2001, US patent 6326619

[18] WRIGHT, S.I., *et al.*, *Chemical prefiltering for Phase Differentiation via Simultaneous Energy Dispersive Spectrometry and Electron Backscatter Diffraction*, 2004, US patent 6835931

[19] DAY, A.P., and QUESTED, T.E., Comparison of grain imaging and measurement using orientation and colour orientation contrast imaging, electron back scatter pattern and optical methods, *J. Microscopy*, **195** (1999), pp. 186-196

[20]   ASTM E 3, *Standard Guide for Preparation of Metallographic Specimens*

[21]   ASTM E 1558, *Standard Guide for Electrolytic Polishing of Metallographic Specimens*

[22]   Application note *Specimen Preparation for Electron Backscatter Diffraction (EBSD) Analysis*, prepared by TSL (http://new.ametek.com/content-manager/files/EDX/specimenpreparation.pdf)

ICS 71.040.50

Price based on 43 pages

This page has been intentionally left blank

BS ISO
24173:2009

BSI - British Standards Institution

BSI is the independent national body responsible for preparing British Standards. It presents the UK view on standards in Europe and at the international level. It is incorporated by Royal Charter.

Revisions

British Standards are updated by amendment or revision. Users of British Standards should make sure that they possess the latest amendments or editions.

It is the constant aim of BSI to improve the quality of our products and services. We would be grateful if anyone finding an inaccuracy or ambiguity while using this British Standard would inform the Secretary of the technical committee responsible, the identity of which can be found on the inside front cover. Tel: +44 (0)20 8996 9000. Fax: +44 (0)20 8996 7400.

BSI offers members an individual updating service called PLUS which ensures that subscribers automatically receive the latest editions of standards.

Buying standards

Orders for all BSI, international and foreign standards publications should be addressed to Customer Services. Tel: +44 (0)20 8996 9001. Fax: +44 (0)20 8996 7001 Email: orders@bsigroup.com You may also buy directly using a debit/credit card from the BSI Shop on the Website http://www.bsigroup.com/shop

In response to orders for international standards, it is BSI policy to supply the BSI implementation of those that have been published as British Standards, unless otherwise requested.

Information on standards

BSI provides a wide range of information on national, European and international standards through its Library and its Technical Help to Exporters Service. Various BSI electronic information services are also available which give details on all its products and services. Contact Information Centre. Tel: +44 (0)20 8996 7111 Fax: +44 (0)20 8996 7048 Email: info@bsigroup.com

Subscribing members of BSI are kept up to date with standards developments and receive substantial discounts on the purchase price of standards. For details of these and other benefits contact Membership Administration. Tel: +44 (0)20 8996 7002 Fax: +44 (0)20 8996 7001 Email: membership@bsigroup.com

Information regarding online access to British Standards via British Standards Online can be found at http://www.bsigroup.com/BSOL

Further information about BSI is available on the BSI website at http://www.bsigroup.com

Copyright

Copyright subsists in all BSI publications. BSI also holds the copyright, in the UK, of the publications of the international standardization bodies. Except as permitted under the Copyright, Designs and Patents Act 1988 no extract may be reproduced, stored in a retrieval system or transmitted in any form or by any means – electronic, photocopying, recording or otherwise – without prior written permission from BSI.

This does not preclude the free use, in the course of implementing the standard, of necessary details such as symbols, and size, type or grade designations. If these details are to be used for any other purpose than implementation then the prior written permission of BSI must be obtained.

Details and advice can be obtained from the Copyright and Licensing Manager. Tel: +44 (0)20 8996 7070 Email: copyright@bsigroup.com

BSI Group
Headquarters 389
Chiswick High Road,
London, W4 4AL, UK
Tel +44 (0)20 8996 9001
Fax +44 (0)20 8996 7001
www.bsigroup.com/
standards